



BTO 2016.042 | June 2016

## **BTO report**

Research pilot of rapid filtration at Velddriel: iron, manganese and ammonium removal



# BTO

## Research pilot of rapid filtration at Velddriel: iron, manganese and ammonium removal

BTO 2016.042 | June 2016

### Project number

400378

### Project manager

K.J. (Klaasjan) Raat

### Client

BTO - Thematic research - Water and energy

### Quality Assurance

E.R. (Emile) Cornelissen

### Author(s)

D. (Dirk) Vries and C. (Cheryl) Bertelkamp

### Sent to

This report is distributed to BTO-participants and is public

**Year of publishing**  
2016

### More information

dr.ir. Dirk Vries  
T 671  
E [dirk.vries@kwrwater.nl](mailto:dirk.vries@kwrwater.nl)

### Keywords

PO Box 1072  
3430 BB Nieuwegein  
The Netherlands

T +31 (0)30 60 69 511  
F +31 (0)30 60 61 165  
E [info@kwrwater.nl](mailto:info@kwrwater.nl)  
I [www.kwrwater.nl](http://www.kwrwater.nl)

The logo for KWR (Watercycle Research Institute) features the letters 'KWR' in a bold, blue, sans-serif font. The 'K' and 'W' are connected, and the 'R' is slightly separated.

Watercycle  
Research  
Institute

BTO 2016.042 | June 2016 © KWR

All rights reserved.

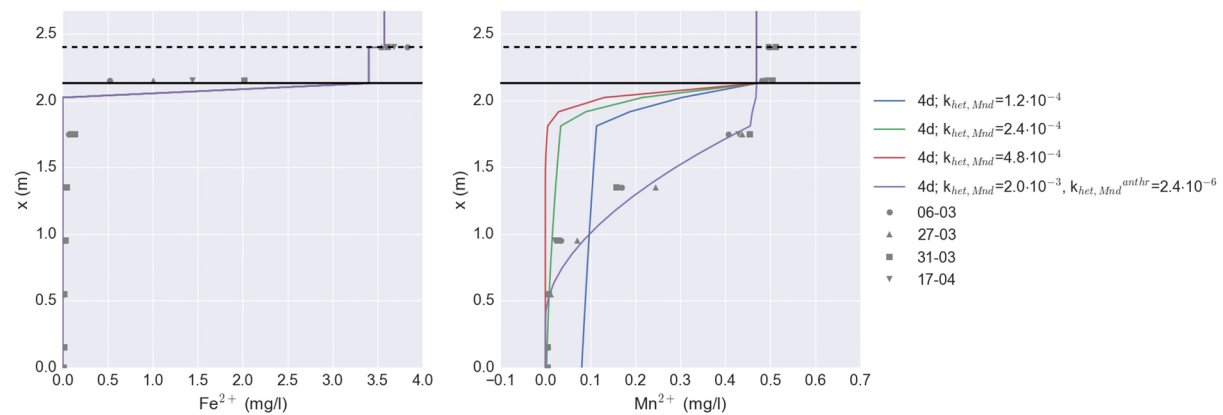
No part of this publication may be reproduced, stored in an automatic database, or transmitted, in any form or by any means, be it electronic, mechanical, by photocopying, recording, or in any other manner, without the prior written permission of the publisher.

## BTO Managementsamenvatting

### Resultaten met uitgebreid model voor verwijdering mangaan, ijzer en ammonium bieden twee opties voor verbetering snelfiltratie Velddriel

Auteur(s) dr.ir. D. (Dirk) Vries en dr.ir. C. (Cheryl) Bertelkamp

Om de verwijdering van ijzer, mangaan en ammonium in de snelfilters van WPB Velddriel beter te kunnen beschrijven is een bestaand model voor ijzer- en mangaanverwijdering in snelfilters uitgebreid met twee mechanismes: dubbellaagsfiltratie en nitrificatie. Simulaties met dit uitgebreide model laten zien dat met twee aanpassingen in het operationele beheer van de filters de ijzer/mangaanverwijdering mogelijk verder te verbeteren is. Deze aanpassingen zijn (i) het conditioneren van het beluchte water om de pH te verhogen (ten behoeve van verbeterde mangaanverwijdering) en (ii) het verlengen van de verblijftijd in het filterbed door het debiet te verlagen. Hierdoor kan de terugspoelfrequentie worden verlaagd en daarmee de looptijd van het filter verlengd. Dit maakt wel een groter filteroppervlak nodig om dezelfde productiecapaciteit te behouden. Experimentele en modelleerresultaten laten zien dat een deel van het filter (de laag vlakbij de bodem) van WPB Velddriel niet effectief bijdraagt aan de verwijdering van mangaan. Dit kan een indicatie zijn dat de filterbedhoogte verkleind zou kunnen worden, maar het is nog onduidelijk of deze reservecapaciteit op de langere termijn wel nodig is. Aanvullende lange-termijn experimenten zijn nodig om de verzadiging van deze laag verder te onderzoeken.



De invloed van heterogene oxidatiesnelheid op de ijzer- (links, horizontale as) en mangaanprofielen (rechts, horizontale as) over de hoogte van het filter, gemeten vanaf de bodem (verticale as) volgens een simulatie van 4 dagen looptijd bij verschillende oxidatiesnelheden (gekleurde lijnen). Het dubbellaags filter heeft de grenslaag van antraciet en zand op 170 cm, de bovenste laag bestaat uit antraciet. De zwarte horizontale lijn geeft de bovenkant van het filterbed weer, de onderbroken zwarte lijn de hoogte van de bovenwaterstand. Het model beschrijft het profiel van mangaan over het filterbed het beste (paarse lijn, rechts) bij de aanname dat de heterogene oxidatiesnelheid afhankelijk is van het filtermateriaal.

### Belang: het vinden van optimale procescondities voor ijzer- en mangaanverwijdering

Zandfilters verwijderen doorgaans in voldoende mate ijzer en mangaan, maar in een aantal gevallen gaat de prestatie van filters sneller achteruit dan voorzien. Hierdoor moeten eerder (kostbare) onderhoudsmaatregelen worden getroffen. Door een onvolledige mangaanverwijdering in de snelfilters op locatie Velddriel, trof Vitens in het verleden mangaanoxides aan in de nageschakelde reactor van de pelletontharding.

### Aanpak: uitbreiden bestaand model met nitrificatie en dubbellaagsfiltratie

Een in eerder BTO onderzoek (BTO 2014.047) ontwikkeld chemische proces- en transportmodel voor ijzer-, mangaan- en ammoniumverwijdering is verbeterd. Dit snelfiltermodel is uitgebreid met twee mechanismen: de verwijdering met dubbellaagsfiltratie en nitrificatie. Data van locatie Velddriel zijn gebruikt om dit model verder te ontwikkelen. Met modelsimulaties is vervolgens onderzocht welke bedrijfsvoeringsparameters het meest geschikt zijn om de ijzer- en mangaanverwijdering in Velddriel verder te optimaliseren.

### Resultaten: meer kennis over het effect van sorptie parameters en heterogene oxidatiekinetiek

De resultaten van deze studie laten zien dat de adsorptiecapaciteiten van verschillende filtermaterialen (bijv. ijzergecoat zand en antraciet) niet gelijk zijn. Ook verschilt de snelheid van heterogene mangaanoxidatie voor diverse materialen: voor zand met een mangaanoxidecoating is deze snelheid hoog, voor antraciet bijna verwaarloosbaar. Het model voor nitrificatie moet nog verder worden getoetst met metingen.

Om de verwijdering van ijzer en mangaan te verbeteren is kan de bedrijfsvoering op twee manieren worden aangepast: (i) het conditioneren van het beluchte water om de pH te verhogen, (ii)

verlengen van de verblijftijd in het filterbed door het verlagen van het debiet (als dat mogelijk is gezien de te leveren capaciteit) of het verhogen van de filterbedhoogte. Hierdoor kan de terugspoelfrequentie verlaagd worden en daarmee de looptijd van het filter verlengd.

Experimentele en modelleerresultaten laten zien dat een deel van het filter (de zone net boven de bodem) niet effectief bijdraagt aan de verwijdering van mangaan. Dit impliceert dat de filterbedhoogte verkleind zou kunnen worden, met als nadeel dat er geen of minder reservecapaciteit voor mangaanverwijdering rest. Aanvullende lange-termijn-experimenten zijn nodig om te onderzoeken of, en zo ja, hoe snel deze ruimte wordt ingenomen door mangaanoxiden.

### Implementatie: aanpassing van de bedrijfsvoering voor betere ijzer/mangaanverwijdering

De voorgestelde aanpassingen (conditioneren van het beluchte water, verlagen van het debiet of verhogen van de filterbedhoogte) kunnen direct in de praktijk worden toegepast, bij voorkeur in een experimentele setting met voldoende aandacht voor monitoring van de effecten. Het is aan te bevelen het model voor nitrificatie nog verder te toetsen en aanvullende lange-termijn-experimenten te doen om te onderzoeken of, en zo ja, hoe snel de "reserve" ruimte in het filterbed wordt ingenomen door mangaanoxiden.

### Rapport

Dit onderzoek is beschreven in rapport *Research pilot of rapid filtration at Velddriel: iron, manganese and ammonium removal* (BTO-2016.042).

Een deel van het experimentele onderzoek uit deze studie is onderdeel van de publicatie "*Iron and manganese removal: recent advances in modelling treatment efficiency by rapid sand filtration*" (Vries et al., ingediend bij Water Research).



# Voorwoord

Met de resultaten van voorgaand BTO-speerpuntonderzoek nog nat op papier, is eind 2014 een projectplan neergezet met de ambitie om modelschattingen te concretiseren naar stuurparameters en handvatten voor bedrijfsvoering van snelfilters (de zuivering bovengronds) en verwijdering van ijzer en/of mangaan in de ondergrond. Het idee was toentertijd dat deze stuurparameters richting zouden geven aan de vraag wanneer en op welke wijze ondergrondse zuivering gecombineerd moest worden met de bovengrondse zuivering dusdanig dat daar aan efficiëntie (bijv. minder spoelwaterverlies) werd gewonnen zonder in te boeten op effectiviteit (behoud van de onberispelijke kwaliteit van drinkwater).

Het projectplan is de aanzet geweest om het model voor de ondergrondse als ook bovengrondse zuivering onder de loep te nemen, alvorens handvatten te formuleren. Dit heeft geleid tot afzonderlijke pilots (voor ondergrond en bovengrond). Het pilotonderzoek ten aanzien van snelfiltratie is belicht in voorliggend werk. Het pilotonderzoek bevatte een uitgebreid meetprogramma, waarvoor we graag de betrokkenen vanuit Vitens van harte willen bedanken:

- Frank Schoonenberg (begeleider van dit onderzoek)
- Martijn Tas
- Patrick Teunissen
- Jan van de Kamp
- Gerrit-Jan Zweere

Jullie inzet, bijdrage aan inhoudelijke discussies en inventieve oplossingen voor bemonstering van de filterketels was van groot belang voor het onderzoek, met name voor de kalibratie en toetsing van het ontwikkelde model. Daarnaast een woord van dank voor het Vitens-lab bij de analyse van de grote set aan monsters.

Graag willen we ook enkele (ex)-collega's bij naam noemen: Benjamin van den Akker, die veel werk heeft verzet in de modelvorming, Bas Hofs, mede-begeleider van dit onderzoek, Paul van der Wielen voor de interpretatie van de qPCR-resultaten en Bas Wols die tijdens een drukke periode heeft ingesprongen bij het simuleren van de effecten van diverse nitrificatiemodelparameters.

Tenslotte, voorliggend werk biedt misschien niet alle antwoorden op de gestelde kennisvragen. De studie heeft wel de kennis over het proces verbeterd. Deze kennis is vervat in een verbeterd model die de waterkwaliteit van snelfiltraat (ook van dubbellaagsfilters) kan voorspellen, waardoor de stap naar concrete stuurparameters en modelgebaseerde sturing in de zuivering een stap dichterbij is gebracht. We wensen de lezer een inspirerende leeservaring.

# Summary

In order to quantitatively describe the start-up and operation of rapid sand filters (RSF), an existing model for iron and manganese removal and nitrification was improved. Model development was supported by a measurement program at the production site Velddriel (Vitens) where pre-aerated dual media filtration is present as a first treatment step. Two mechanisms were added to the RSF model: removal by dual media filtration and nitrification. Furthermore, qPCR and ATP analysis have been carried out in order to assess nitrification and biological activity across the filter bed. Results show that the model is sensitive to the model parameters corresponding to adsorption parameters, filtration run time and heterogeneous oxidation kinetics. Iron coated sand and anthracite adsorb differently as shown by adsorption isotherm determination and subsequent model simulation. The heterogeneous manganese oxidation rate constant was calibrated to a high value for manganese oxide coated sand and almost negligible for anthracite. The effect of backwashing on the microbial population present in the filter bed could not be determined due to insufficient data. Process parameters that can be adjusted to improve iron and manganese removal are: (i) conditioning the aerated water to increase pH to improve manganese removal (possibly at the cost of faster pressure built-up due to iron oxide flocs) and (ii) increasing the residence time in the filter bed by lowering the flow capacity in the case production capacity is more than sufficient. This way, the backwash frequency can be lowered (case (ii)), or the life time of the filter material can be prolonged (case (i)). Experimental and modeling results seem to indicate that the Velddriel filter has a substantial removal capacity due to the amount of iron coated sand, since the bottom region of the filter is - at the time of the measurement campaign - not effectively contributing to the removal. Long(er) term experiments are needed to assess whether this redundant capacity is needed in a later phase to further delay or even prevent the breakthrough of manganese.

# Contents

<b>Summary</b>	<b>3</b>
<b>Contents</b>	<b>5</b>
<b>1 Introduction</b>	<b>6</b>
1.1 Background	6
1.2 Project description	7
1.3 Procedure	7
<b>2 Modelling and measurement programme at Velddriel</b>	<b>9</b>
2.1 Modelling the removal processes by RSF	9
2.2 Validation programme by field data from Velddriel	19
<b>3 RSF model results and validation</b>	<b>21</b>
3.1 Velddriel data	21
3.2 Modelled iron, ammonium and manganese removal compared with Velddriel and Holten data	23
3.3 Python-PHREEQC RSF model: preliminary results	37
<b>4 Conclusions and recommendations</b>	<b>39</b>
4.1 Conclusions	39
4.2 Recommendations	39
<b>5 Literature</b>	<b>42</b>
<b>Attachment I PHREEQC code blocks</b>	<b>44</b>
<b>Dual media filtration and nitrification</b>	<b>44</b>
Dual media filtration model, PHREEQC code	44
Nitrification	45
	46
Transport model in Python, linked to PHREEQC for speciation	46
<b>Attachment II Additional figures AOA and AOB analysis</b>	<b>48</b>
<b>Attachment III Additional figures evolution of iron and manganese removal</b>	<b>50</b>
Velddriel, single medium filter model	50
Velddriel, double media filter model	51
Holten, dynamic evolution of filtration	52

# 1 Introduction

## 1.1 Background

The optimal operational conditions for rapid sand filtration to treat groundwater and remove iron, manganese and ammonium are difficult to predict. In practice, these processes work well under different circumstances: the pH of the raw water can range from 6.0 to about 8.0, manganese levels can vary an order of magnitude from 0.1 mg/L to about 1.0 mg/L and also the iron concentration levels may differ from 2 to 23 mg/L. Additionally, ammonium removal requires specific biological activity. For all these compounds, efficient removal requires adsorption and transport along (metal) coated sand particles and oxygen. Complexity is increased by the diversity of process conditions at different actual production facilities: the facilities that use rapid sand filtration (RSF) may differ among each other. While some facilities have filtration units where only one filtration medium (i.e. a single layer of sand) is used for treatment, other units have a double layer consisting of anthracite and sand. The way oxygen is introduced in the treatment process can be different by design: plate aeration, venturi aeration and spray aeration are all commonly used aeration options.

This report focussed on the rapid dual media filters used by Vitens at location Velddriel. Groundwater is abstracted here and treated by rapid dual media (anthracite and sand) pre-filters, softening and rapid dual media (anthracite and sand) post-filters. Subsequently, the water is distributed to the customers. After one to two years of regular operation and filter media replacement, Vitens experienced the breakthrough of manganese from the pre-filter. Manganese oxidized in the subsequently in the cellar and pellet softening reactor, leading to manganese oxides clogging the slits of the reactor caps. Hence, insight in iron and manganese removal was needed to determine if these problems could be circumvented by an adapted process operation. In addition, there were questions about the effectiveness of a dual media filter for the removal of iron/manganese and what the effect would be of backwashing the filter on the iron/manganese removal.

Research questions formulated by Vitens for this specific location were:

1. Is it possible to control iron and manganese removal by adapting process parameters?
2. Is a dual media rapid filter more efficient with respect to iron/manganese removal compared to single medium filter?
3. What is the effect of backwashing of the dual media filter on iron/manganese removal? Will the backwashing result in a mixed bed, i.e. with no separation of the two filter media in a dual media filter?

Insight in the physical, chemical and biological processes that occur during removal of iron and manganese will assist in the operational optimisation and prevention of unintentional operational disturbances or ineffective or counterproductive measures. Indeed, models are particularly useful to integrate the interdependent physical, chemical and biological aspects and processes (Akker, Antoniou, Hartog, Vries, & Hofs, 2014). Also, developed models can, through comparison with actual laboratory or field test data, validate whether the underlying assumptions and level of understanding are sufficiently accurate. Finally, such validated models can provide simulation tools for design, control, optimization and prediction purposes.

## 1.2 Project description

In this study we explored, described and improved the modelling of physical, chemical and biological processes that occur during iron and manganese removal. In previous research projects (Akker et al., 2014; Teunissen, 2007; Vries & Akker, 2013a, 2013b), it was found that iron and manganese removal can be modelled, but validation and testing of adsorption capacity was still limited to the Holten production site case. Moreover, the built up of iron- and manganese (hydroxyl)oxide coating on the filter medium during the early stages of the start-up of RSF has not been explored yet. Additionally, the influence of backwashing was still not quantified and coupled with the (chemical) removal modelling. And finally, nitrification and the ammonium removal dependency on the availability of oxygen coupled to the iron and manganese removal model has not been investigated yet.

In 2013, the following project goals for the above ground treatment (RSF) have therefore been formulated by the project team:

1. what are the rules of thumb for improved treatment in the underground (in-situ treatment) and at the treatment production site such that:
  - a. Iron, manganese and ammonium are removed during a prolonged period while limiting the amount of backwashing;
  - b. The duration time of taking RSFs into production (after e.g. replacement of the filter medium) is decreased by operational measures.
2. Investigate the optimal trade-off between in-situ treatment and treatment with RSF at production sites where above and sub-surface treatment is applied. Deliver model simulation results that support business case calculations of overall removal efficiency versus associated operational costs.

## 1.3 Procedure

To realise the project objectives by modelling, it was assumed that the (final) model was able to:

1. Predict iron, manganese and ammonium removal for a variety of conditions (including process conditions like different (layers of) filter media, bed contact time as well as water quality variations in alkalinity, iron, manganese and ammonium levels) over the full filter bed height;
2. Capture the evolution of iron and manganese removal during start-up of a RSF, where in general, it takes about one month to accomplish the (almost) complete removal of manganese and a few days for the removal of iron;
3. Simulate the effect of backwashing on removal capacity of iron(II), manganese(II) and ammonium during operation and during start-up.

Hence, corresponding project activities have been formulated:

- A1. Improve the model on iron and manganese removal, incorporate nitrification and validate the model on removal characteristics of Fe, Mn and  $\text{NH}_4$ ;
- A2. Develop (or extend the current model with) a dynamic model for start-up of RSFs;
- A3. Incorporate the efficacy of backwashing frequency and intensity in model;

In chapter 2 and 3, we outline the approach of activities A1 to A3 by describing the procedure and results, respectively. Part of activity A1 is conducted within the BTO project 'Onderste korrel boven' (Vries, Bertelkamp, Akker, & Hofs, 2016), that is, experiments to determine adsorption characteristics of the filter material in Velddriel and model validation with field data. An analysis of the optimal trade-off between in-situ treatment and treatment with RSF is

given in a separate chapter. Table 1-1 shows how the chapters and sections are linked to project activities A1, A2 and A3.

TABLE 1-1: READING GUIDE

Chapter	What is described	Activity and corresponding paragraph
2: Modelling and measurement programme at Velddriel	Methodology, procedure and model changes	A1: 2.1 Modelling the removal processes by RSF
3: RSF model results and validation	Discussion of model simulation results and measurements at Velddriel	A2 and A3: 2.1.4 Metal oxide accumulation and backwashing efficacy (A2 – A3) A1: 3.1 Velddriel data A1: 3.2 Modelled iron, ammonium and manganese removal compared with Velddriel and Holten data A2: 3.3 Modelled start-up of RSF A3: 3.4 Backwashing efficacy
4: Conclusions and recommendations		A1 to A3

## 2 Modelling and measurement program at Velddriel

### 2.1 Modelling the removal processes by RSF

The RSF model as described in BTO report 2014.047 (Akker et al., 2014) was used as a starting point. In the Introduction of this report, paragraph 1.3, it has been observed that a quantitative description of the removal of iron, manganese and ammonium required a model that was able to:

1. predict iron, manganese and ammonium removal for a variety of conditions, including process conditions (like flow rate and bed height) as well as water quality variations in alkalinity, iron, manganese and ammonium levels over the full filter bed height;
2. capture the evolution of iron and manganese removal during start-up of a RSF, where especially the achievement to completely remove manganese(II) can take more than a few weeks, leading to production costs;
3. simulate the effect of backwashing on removal capacity during operation and during start-up.

At the start of this research study, aims (2) and (3) were not fulfilled and the model could only predict iron and manganese removal when adsorption isotherm data are available. Furthermore, the existing model has been developed for single medium rapid sand filtration. Additionally, the RSF model was not tested yet at multiple drinking water production sites.

Hence, the project activities A1 (model improvements, addition of nitrification and validation), A2 (accumulation of metal oxides), and A3 (modelling backwashing efficacy) have been carried out. These activities are described in the subsequent paragraphs in more detail, where corresponding activities have been abbreviated and placed between brackets.

#### 2.1.1 Parametrization and validation of iron and manganese removal (A1)

The existing, (see (Akker et al., 2014)) RSF model for iron and manganese removal (say RSF model v1.0):

- was parametrized in homogeneous oxidation and corresponding model parameters (oxidation constants for iron and manganese, residence time, dissolved oxygen concentration level, reaction stoichiometry);
- was parametrized in heterogeneous oxidation and corresponding model parameters (amount of hydrous ferric (oxy)oxides like ferrihydrite and manganese oxides, like birnessite  $\text{Na}_{0.3}\text{Ca}_{0.1}\text{K}_{0.1}(\text{Mn}^{4+}, \text{Mn}^{3+})_2\text{O}_4 \cdot 1.5\text{H}_2\text{O}$ ), adsorption isotherm parameters, heterogeneous oxidation rate constants, homogeneous porosity throughout the filter bed and reaction stoichiometry) for a filter filled with one filter medium material.
- was extended with nitrification as a removal mechanism for ammonium;

Although for RSF model v1.0, much has been simplified by e.g. the assumptions of formed metal oxides (assuming HFO as  $\text{Fe}_2(\text{OH})_3$  and manganese oxides in the form of completely oxidised species  $\text{MnO}_2$ ), there was still a discrepancy between total amount of necessary model parameters versus experimental parameters that can be obtained in practice.

Hence for validation purposes, we have made more simplifying assumptions:

- (literature) values for homogeneous oxidation are used throughout this study, also because of limited availability of measurement data in the supernatant level;
- $\text{Fe}^{+2}$  and  $\text{Mn}^{+2}$  ions will bind to only HFO (hydrrous ferric oxides), because characterization of metal oxide (at different depths) is often not available, whereas (limited) data of adsorption characteristics of (non-characterised) filter material is available. In the case of RSF at Velddriel, adsorption data is collected but filter material is not characterised further with respect to the crystalline state and composition of HFO and manganese oxides. Hence adsorption of iron and manganese is assumed to take place at HFO and the RSF model is simulated until the (quasi) steady state that adsorbed iron and manganese does not change at different filter depths. The downside of this approach is that the adsorption of manganese may be underestimated by the model due to the competition with iron(II) regarding HFO binding sites;
- Biological iron and manganese removal is neglected and assumed to be part of (characterised) heterogeneous adsorption by incorporating the contribution of (possible) biological catalysis in the heterogeneous reaction rate constant.

Next to simplifying assumptions, the filter model has been extended to incorporate nitrification (see Paragraph 2.1.3) and two layers of filter media in order to have correspondence with the RSFs at production site Velddriel (see Paragraph 2.1.2). An overview of used parameters of the base model (without nitrification) is given in Table 2-1 and Table 2-5 (nitrification). Please note that, in addition to testing the influence of the adsorption isotherms and heterogeneous constant  $k_{\text{het}}$  on the model outputs, also the influence of filtration velocity (flow) and the dispersivity constant is checked.

TABLE 2-1: MODEL PARAMETERS FOR IRON AND MANGANESE REMOVAL USED IN THIS STUDY. PARAMETERS IN BOLDFACE HAVE BEEN INVESTIGATED IN THIS STUDY

Model parameter	Notation	PHREEQC parameter	RSF v1.0	This study	Validation
Homogeneous iron oxidation constant	$k_{\text{Fe, hom}}$	Fd_ox_hom	Literature	Value as in RSF v1.0	no
Homogeneous manganese oxidation constant	$k_{\text{Mn, hom}}$	Mnd_ox_hom	Literature	Value as in RSF v1.0	no
Porosity	$\phi$	-	Estimated from RSF specific characteristics		no
Superficial flow velocity	$v$	-	Value calculated from WPB specific process conditions	Production flow ( $Q_p$ ), $Q_p + 33\%$ and $Q_p - 33\%$	no
Dispersivity <sup>1</sup>	dispersivity	dispersivities	Default value of 0 m is assumed.	[0, 0.1 and 0.5] m	no
<b>Heterogeneous iron oxidation constant on HFO</b>	$k_{\text{Fe, het}}$	Fd_ox_hfo	Literature	3.0 single layer	no

<sup>1</sup> 'Dispersivity' defines the tendency to mix with adjacent cells in advective-dispersive transport simulations (units in meter)

Heterogeneous manganese oxidation constant on HFO	$k_{Mn,het}$	Mnd_ox_hfo	Literature ( $2.4 \cdot 10^{-4}$ )	73.0 double layer, 4 values tested [ $2.4 \cdot 10^{-4}$ , $2.4 \cdot 10^{-6}$ , $2.0 \cdot 10^{-3}$ ]	no
Heterogeneous manganese oxidation constant on birnessite	$k_{Mn,het}$	Mnd_ox_birn	Literature	neglected	no
Freundlich constant ( $Fe^{+2}$ at HFO)	$K_f$	$\log_k^*$	Literature and characterisation filter material of WTP Holten	Characterised value (filter material RSF Velddriel) at different depths (see Table 2-2)	several locations, see (Vries et al., 2016)
Freundlich constant ( $Fe^{+2}$ at HFO)	(1/n)	$1/n^*$			
Freundlich constant ( $Mn^{+2}$ , at HFO)	$K_f$	$\log_k^*$			
Freundlich constant ( $Mn^{+2}$ , at HFO)	(1/n)	$1/n^*$			
Freundlich constant ( $Mn^{+2}$ , at birnessite)	$K_f$	$\log_k^*$		neglected	n.a.
Freundlich constant ( $Mn^{+2}$ , at birnessite)	(1/n)	$1/n^*$		neglected	n.a.
Biological iron removal parameters		Mumax, Y, m, K	Literature	neglected	n.a.**

\* see the corresponding reactions written in the `surface_species` block.

\*\* at the exception of ATP measurements.

### 2.1.2 Extension of RSF model with multiple filter media layers (A1)

To allow for heterogeneous oxidation in more than one layer, the (single layer) PHREEQC model was modified by:

- adding a separate 'phase species' that acts as a surface complexation agent;
- specifying the Freundlich isotherm values for the added phase species;
- specifying the cells which will correspond to the layer region at which the different filter medium is present.

For Velddriel, the dual layer model is simulated with a filter layer boundary at different depths corresponding to the boundary between the anthracite and sand layer. Both models are simulated by assuming a clean bed at the start of the filtration period until a filtration run time of 31 days is simulated.

TABLE 2-2: OVERVIEW OF SIMULATION SETTINGS FOR THE SINGLE MEDIUM AND THE DUAL MEDIA RSF MODEL. SAMPLES FROM THE UPPER LAYER REGION WAS ESTIMATED AT [0.0 - 0.75 M], MIDDLE LAYER REGION AT [0.75 - 1.25 M] AND LOWER REGION AT [1.5 - 2.0 M]. THE FREUNDLICH CONSTANTS ARE

DETERMINED BY ADSORPTION ISOTHERM EXPERIMENTS ( PROCEDURE IS DESCRIBED IN SCHOONENBERG-KEGEL (2015) AND VRIES ET AL. (2016). VRIES ET AL.

	Simulation name	Boundary layer depth [m]	Freundlich constants for iron(II) and manganese(II)			
			Iron(II) K <sub>f</sub> (mg/g) / (mg/L) <sup>1/n</sup>	1/n	Manganese(II) K <sub>f</sub> in (µg/g) / (µg/L) <sup>1/n</sup>	1/n
Single layer model	• U*	n.a.**	• 1.58 (U)	• 0.540 (U)	• 1.04 (U)	• 0.814 (U)
	• M*		• 0.42 (M)	• 0.225 (M)	• 0.19 (M)	• 0.369 (M)
	• L*		• 0.37 (L)	• 0.228 (L)	• 0.13 (L)	• 0.507 (L)
Dual layer model	• 32 cm	• 0.32 m	1.58	0.540	1.04	0.814
	• 43 cm	• 0.43 m	(anthracite),	(anthracite),	(anthracite),	(anthracite),
	• 100 cm	• 1.00 m	0.42 (IOCS)	0.225 (IOCS)	0.19 (IOCS)	0.369 (IOCS)

\*: U: upper, M: middle, L: lower.

\*\* : n.a.: not applicable.

Excerpts of the PHREEQC code blocks are given in Attachment I (Velddriël case) Figure I-1, Figure I-2, and Figure I-3. In addition, different values of the heterogeneous manganese oxidation constant ( $k_{Mn,het}$ ) are tested, assuming a dual media filtration (DMF) model with a sand boundary layer at 32 cm (measured from the top of the filter bed):  $2.4 \cdot 10^{-4}$  (value from Davies & Morgan (1989)),  $4.8 \cdot 10^{-4}$  and  $2.0 \cdot 10^{-3} \text{ s}^{-1}$  for *both* anthracite and sand filter layers, and one simulation where the heterogeneous manganese oxidation constant is high ( $2.0 \cdot 10^{-3} \text{ s}^{-1}$ ) for the sand layer, and very low for the anthracite layer ( $2.4 \cdot 10^{-6} \text{ s}^{-1}$ ).

### 2.1.3 Incorporation of nitrification (A1)

Nitrification is included in the current RSF model by implementing the equations as proposed by van der Aa et al., (2002). The model consists of ammonia removal by two species of bacteria each consisting of specific growth characteristics: Nitrosomonas convert ammonia into nitrite and Nitrospira bacteria convert nitrite into nitrate. This model is set-up like many biological growth and consumption models: the specific growth rate of the micro-organism increases with available substrate and other rate-limiting compounds according to a saturation curve. In this model, the saturation curve is determined by half-saturation constants for phosphate, ammonium and oxygen and a specific maximum growth rate constant. Consumption of substrate is determined by the available biomass and a yield factor. A higher ratio of (maximal) growth rate versus biomass yield factor ( $\mu/Y$ ) means that more substrate (here: ammonium, oxygen or phosphate) is removed for accumulation of biomass. A maintenance rate constant determines the point at which bacteria do not grow exponentially but reaches equilibrium in biomass accumulation, death rate and energy needed for energy. The model is validated with data collected from a filtration unit treating surface water.

Further assumptions and model characteristics are listed below:

- The bacteria are assumed to be immobile and already present in biofilms that cover the filter media in the RSF. Desorption of bacteria during their growth is allowed (parameter  $d_1$ , (Aa et al., 2002; Willemse & Dijk, 1994)), but desorption of the current biomass ( $d_2$ ) is neglected because the maintenance constant ( $b_{Ns}$ ) has mathematically exactly the same influence as  $d_2$  ;
- The potential growth rate ( $\mu$ ) is determined by the limiting substrate, i.e. ammonium, phosphate or oxygen. In case of complete nitrification the ammonium, respectively nitrite concentration is the limiting substrate for the Nitroso, respectively Nitrospira-bacteria;
- Temperature and pH dependence is incorporated, according to the model as proposed by Aa et al. (2002);
- The influence of diffusion from the bulk liquid into the biofilm is not incorporated.

The model parameter values are collected and varied using two data sources (Aa et al., 2002; Rietveld, Helm, Schagen, Aa, & Dijk, 2008) as a basis. The values as reported in these literature sources are shown in Table 2-3 and Table 2-4 for the species Nitrosomonas and Nitrospira, respectively. The corresponding PHREEQC code is included in Attachment I.

The values used for various simulations are shown in Table 2-5, exploiting the estimated range of values as reported in Aa et al. (2002) and Willemse & Dijk (1994). For the dispersion coefficient, we allow a maximal value that is double as large as would be generally assumed by a rule of thumb that this value should be (maximally) in the order of the grain diameter (Gitis et al., 2010).

TABLE 2-3: GROWTH RATE, MAINTENANCE RATE CONSTANTS AND BIOMASS YIELD VALUES OF THE SPECIES NITROSOMONAS

Nitrosomonas	Maximal specific growth rate	Maintenance rate constant	Biomass yield factor	Maximal consumption ratio
PHREEQC tag	$\mu_{Max15\_Ns}$	$b_{Ns}$	$Y_{Ns}$	$\mu_{Max15\_Ns}/Y$
unit	1/s	1/s	(g d.s./m <sup>3</sup> )/(mg NH <sub>4</sub> -N/L)	(mg NH <sub>4</sub> -N/L)/(s g d.s./m <sup>3</sup> )
Most likely value <sup>2</sup>	3.70E-05	1.00E-06	0.12	3.08E-04
Min. value <sup>1</sup>	1.70E-05	4.60E-07	0.04	4.25E-04
Max. value <sup>1</sup>	7.90E-05	4.00E-06	0.17	4.65E-04
Value in STIMELA	5.00E-06	2.00E-07	0.15	3.33E-05

<sup>2</sup> Aa et al. (2002). These values are referred to as Van der Aa [avg] in figures.

TABLE 2-4: GROWTH RATE, MAINTENANCE RATE CONSTANTS AND BIOMASS YIELD VALUES OF THE SPECIES NITROSPIRA

<b>Nitrospira</b>	<b>Maximal specific growth rate</b>	<b>Maintenance rate constant</b>	<b>Biomass yield factor</b>	<b>Maximal consumption ratio</b>
<i>PHREEQC tag</i>	muMax15_Ns	b_Ns	Y_Ns	muMax15_Ns/Y
<i>Unit</i>	1/s	1/s	(g d.s./m3)/(mg NH4-N/L)	(mg NH4-N/L)/ (s g d.s./m3)
Mean value (Aa et al., 2002)	1.00E-06	3.00E-06	0.05	6.00E-05
Min. value (Aa et al., 2002)	4.60E-07	7.30E-07	0.04	1.83E-05
Max. value (Aa et al., 2002)	4.00E-06	4.80E-06	0.06	8.00E-05
Value in STIMELA	2.00E-07	9.00E-06	6.00E-02	1.50E-04

TABLE 2-5: OVERVIEW OF NITRIFICATION MODEL PARAMETER CONSTANTS

	Nitrosomonas					Nitrospira			pH correction	Desorption coefficient	Dispersion
	Max. specific growth rate	Maintenance rate constant	Biomass yield factor	Monod constant for NH <sub>4</sub>	Initial condition	Max. specific growth rate	Maintenance rate constant	Biomass yield factor			
<i>PHREEQC tag</i>	muMax15_Ns	b_Ns	Y_Ns	KsNH4_Ns_0		b_Nb	muMax15_Nb	Y_Nb		d1	a
<i>unit</i>	1/s	1/s	(g d.s./m <sup>3</sup> )/ (mg NH <sub>4</sub> -N/L)	mg/L	g d.s./m <sup>3</sup>	1/s	1/s	(g d.s./m <sup>3</sup> )/ (mg NH <sub>4</sub> -N/L)		1/s	m
1 (Figure 3-11, Figure 3-12)	3.70E-05	1.00E-06	0.12	0.405	0.2	1.00E-06	3.00E-06	0.05	True	0.0	0.0
2	5.00E-06	2.00E-07	0.15	0.405	0.2	2.00E-07	9.00E-06	6.00E-02	True	0.0	0.0
3 (Figure 3-11, Figure 3-12)	3.70E-05	4.00E-06	0.12	0.405	0.2	1.00E-06	3.00E-06	0.05	True	0.0	0.0
4 (Figure 3-11, Figure 3-12)	3.70E-05	2.00E-06	0.12	0.405	0.2	1.00E-06	3.00E-06	0.05	True	0.0	0.0
5	1.70E-05	1.00E-06	0.12	0.405	0.2	1.00E-06	3.00E-06	0.05	True	0.0	0.0
6	7.90E-05	1.00E-06	0.12	0.405	0.2	1.00E-06	3.00E-06	0.05	True	0.0	0.0
7	3.00E-05	1.00E-06	0.12	0.405	0.2	1.00E-06	3.00E-06	0.05	True	0.0	0.0
8 (Figure 3-11, Figure 3-12)	3.70E-05	1.25E-06	0.12	0.405	0.2	1.00E-06	3.00E-06	0.05	True	0.0	0.0
9 (Figure 3-13)	2.60E-05	1.00E-06	0.12	0.2	0.02	1.00E-06	3.00E-06	0.05	True	0.0	0.0
10 (Figure 3-13)	2.05E-05	1.00E-06	0.12	0.1	0.02	1.00E-06	3.00E-06	0.05	True	0.0	0.0
11 (Figure 3-13)	3.70E-05	1.00E-06	0.12	0.405	0.02	1.00E-06	3.00E-06	0.05	True	0.0	0.0
12	3.70E-05	1.00E-06	0.1	0.405	0.02	1.00E-06	3.00E-06	0.05	True	0.0	0.0

13	1.00E-05	1.00E-06	0.12	0.01	0.02	1.00E-06	3.00E-06	0.05	True	0.0	0.0
14	3.70E-05	1.00E-06	0.012	0.405	0.02	1.00E-06	3.00E-06	0.05	True	0.0	0.0
17 (Figure 3-14, Figure 3-15)	<b>1.00E-05</b>	<b>2.00E-07</b>	<b>0.012</b>	<b>0.405</b>	<b>0.02</b>	<b>1.00E-06</b>	<b>3.00E-06</b>	<b>0.05</b>	<b>True</b>	<b>0.0</b>	<b>0.0</b>
18 (Figure 3-14, Figure 3-15)	<b>2.00E-05</b>	<b>2.00E-07</b>	<b>0.012</b>	<b>0.405</b>	<b>0.02</b>	<b>1.00E-06</b>	<b>3.00E-06</b>	<b>0.05</b>	<b>True</b>	<b>0.0</b>	<b>0.0</b>
19	8.00E-06	2.00E-07	0.012	0.405	0.02	1.00E-06	3.00E-06	0.05	True	0.0	0.0
20	5.00E-06	2.00E-07	0.012	0.405	0.02	1.00E-06	3.00E-06	0.05	True	0.0	0.0
21	6.00E-06	2.00E-07	0.012	0.405	0.02	1.00E-06	3.00E-06	0.05	False (0.14)	0.0	0.0
22 (Figure 3-16)	<b>6.00E-06</b>	<b>2.00E-07</b>	<b>0.012</b>	<b>0.405</b>	<b>0.02</b>	<b>1.00E-06</b>	<b>3.00E-06</b>	<b>0.05</b>	<b>True</b>	<b>0.0</b>	<b>0.0</b>
23	6.00E-06	2.00E-07	0.012	0.405	0.02	1.00E-06	3.00E-06	0.05	True	0.15	0.0
24 (Figure 3-16)	<b>6.00E-06</b>	<b>2.00E-07</b>	<b>0.012</b>	<b>0.405</b>	<b>0.02</b>	<b>1.00E-06</b>	<b>3.00E-06</b>	<b>0.05</b>	<b>True</b>	<b>0.3</b>	<b>0.0</b>
25	6.00E-06	2.00E-07	0.012	0.405	0.02	1.00E-06	3.00E-06	0.05	True	0.45	0.0
26	6.00E-06	2.00E-07	0.012	0.405	0.02	1.00E-06	3.00E-06	0.05	True	0.6	0.0
27	6.00E-06	2.00E-07	0.012	0.405	0.02	1.00E-06	3.00E-06	0.05	True	0.02	0.0
28 (Figure 3-16)	<b>6.00E-06</b>	<b>2.00E-07</b>	<b>0.012</b>	<b>0.405</b>	<b>0.02</b>	<b>1.00E-06</b>	<b>3.00E-06</b>	<b>0.05</b>	<b>True</b>	<b>0.05</b>	<b>0.0</b>
29 (Figure 3-16)	<b>6.00E-06</b>	<b>2.00E-07</b>	<b>0.012</b>	<b>0.405</b>	<b>0.02</b>	<b>1.00E-06</b>	<b>3.00E-06</b>	<b>0.05</b>	<b>True</b>	<b>0.02</b>	<b>0.016</b>

#### 2.1.4 ATP and PCR analysis

To assess the amount of biomass present on the sand and in the water samples, ATP analyses were performed according to the method described in (Magic-Knezev & Kooij, 2004).

To determine the amount of ammonia oxidizing bacteria (AOB) and archae (AOA), qPCR analysis was performed on water and sand samples from the dual media filter (Velddriel) and a solubilizing procedure. Samples of the filter material were taken from three regions: 0 – 0.5, 0.75 – 1.25 and 1.5 – 2.0. Water samples were collected from the filter tap points illustrated in Figure 2-2. Samples were obtained at four different time points. A detailed description of the qPCR methodology is presented in (Wielen et al., 2009). These samples were obtained 3 months after the filter material was replaced.

#### 2.1.5 Metal oxide accumulation and backwashing efficacy (A2 – A3)

In this part of the project, the aim was to describe and predict backwashing efficiency in relation to metal oxide accumulation in the form of floc deposits. In order to pursue this aim, differential equations for floc attachment and detachment have to be incorporated. Since PHREEQC is not primarily aimed for integration of differential equations outside the usual `TRANSPORT` and `KINETICS` blocks, it was found necessary to rewrite parts of the existing RSF model into the Python programming language to reduce the spatial and time dependent calculations with respect to floc attachment and detachment, pressure build-up by these flocs (IOCS and MOCS particle size increase) and removal of flocs by shear during backwashing. Models that take into account attachment and detachment of flocs are generally referred to as deep bed filtration models (Gitis, Rubinstein, Livshits, & Ziskind, 2010; Jegatheesan & Vigneswaran, 2005; Maroudas & Eisenklam, 1965) and basically consider the following approaches for calculating deposits of flocs and (breakthrough) of suspended particles (Gitis et al., 2010):

1. Irreversible accumulation (Maroudas & Eisenklam, 1965), where it is assumed that there is only attachment with a deposit rate proportional to the filtration coefficient;
2. Reversible accumulation, where attachment as well as detachment of particles are considered;
3. Multistage accumulation (Gitis et al., 2010), where three stages are defined: (i) a *ripening* stage where a deposit monolayer on filter medium is irreversibly formed, (ii) an *operable* stage, where there is a reversible accumulation of deposits due to filtration and backwashing; and (iii) a *breakthrough* stage where (locally) a certain amount of the deposited material is reached and subsequently causes a halt of further accumulation, eventually leading to breakthrough.

Using the multistage accumulation model, the first step was to model transport and other differential equations in the Python programming language with calls to PHREEQC to calculate the mixing in the supernatant and speciation per cell (filter height at  $x$ ) and per time step  $t$ . As a consequence, an array of  $x_n$  (total number of cells, representing the full bed height) by  $t_n$  (number of time steps) is initialized where a calculation is to be performed for each cell. The amount of homogeneously oxidized iron(II) and manganese(II) in both the supernatant layer and filter bed layer (cells) is obtained by integration over a small time step  $dt$  and using the concentration of iron(II) and manganese(II) of the previous (upper) cell and time step. For each cell, adsorbed iron(II) and manganese(II) are calculated by Freundlich, together with the known total amount of iron and manganese using a root finding technique. Subsequently, speciation is calculated by PHREEQC using a template file with a `SOLUTION`, `REACTION` and `SELECTED_OUTPUT` block. Reactions are set at zero in the `REACTION` block at initialisation. A Python function is then called to fill in the variables for iron(II),

manganese(II), oxygen, etc. and write the result to PHREEQC by the file `model_run.phrq`. After the execution of PHREEQC, the output is written to a file in ASCII text format with `.SEL` extension. The SEL-file has the same output syntax as PHREEQC and can be read by (Python) plotting functions. Figure 2-1 gives a schematic overview of the Python-PHREEQC model setup. Preliminary results are given in Paragraph 3.3.

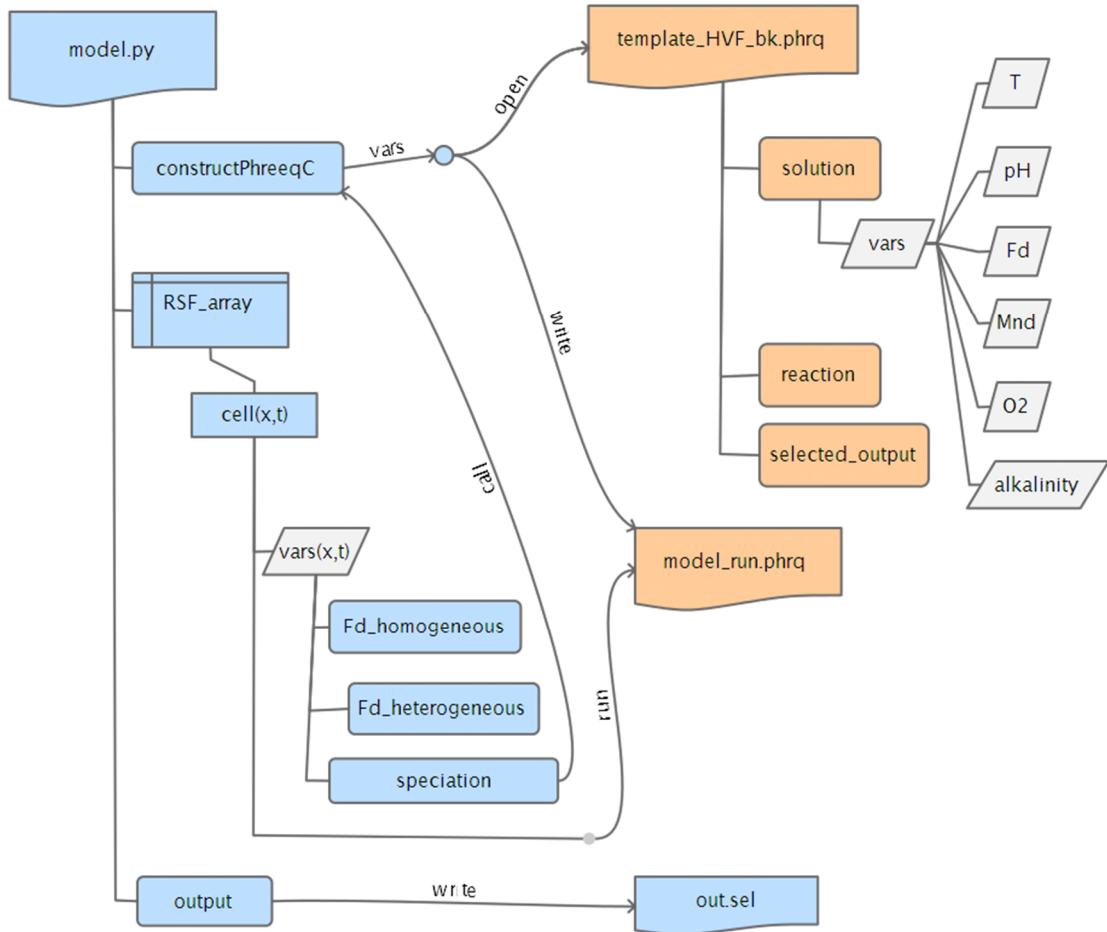


FIGURE 2-1: SCHEMATIC OUTLINE OF PYTHON-PHREEQC MODEL SETUP TO PERFORM TRANSPORT, HOMOGENEOUS AND HETEROGENEOUS OXIDATION CALCULATIONS FOR RSF SIMULATIONS

## 2.2 Validation programme by field data from Velddriel

The groundwater treatment at production site Velddriel consists of the following treatment steps: ground water abstraction, pre-aeration via an inlet and forced aeration, rapid pre-filtration (anthracite/sand), softening, CO<sub>2</sub> conditioning, and rapid post-filtration (anthracite/sand). A schematic overview of the treatment train is presented in Figure 2-1. In this work, focus is aimed at the pre-filtration part. The pre-filter is operated with a nominal flow of 100 m<sup>3</sup>/h and has a backwash frequency of 4 to 5 days, with a backwash filter velocity of 60 m/h.

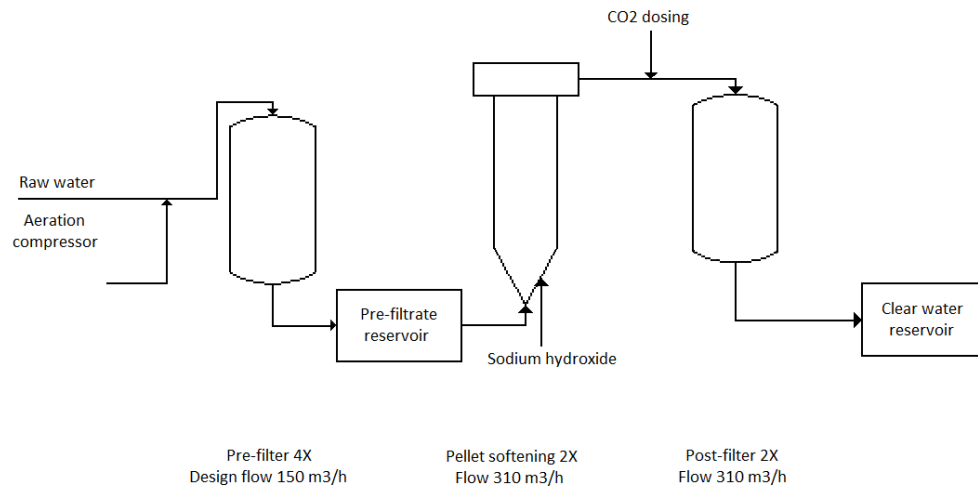


FIGURE 2-2-1: TREATMENT SCHEME WATER PRODUCTION LOCATION VELDDRIEL

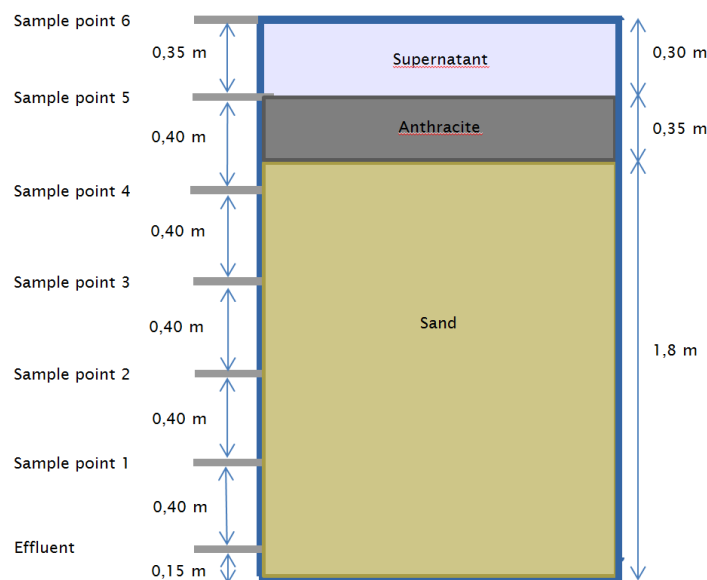


FIGURE 2-2 SCHEMATIC OVERVIEW OF THE PRE-FILTER WITH SAMPLE POINTS

Figure 2-2 presents a schematic overview of a pre-filter at Velddriel. The anthracite layer was characterized by a height of 0.35 m, while the sand layer height was 1.8 m. Six sample points are distributed over the height of the filter bed. To obtain samples, a measuring lance was used. Sample point 5 was located on the boundary of the supernatant and anthracite layer.



### 3 RSF model results and validation

#### 3.1 Velddriel data

Samples were taken according to section 2.1.4 for ATP and qPCR analysis (respectively section 3.1.1 and section 3.1.2).

##### 3.1.1 ATP measurements

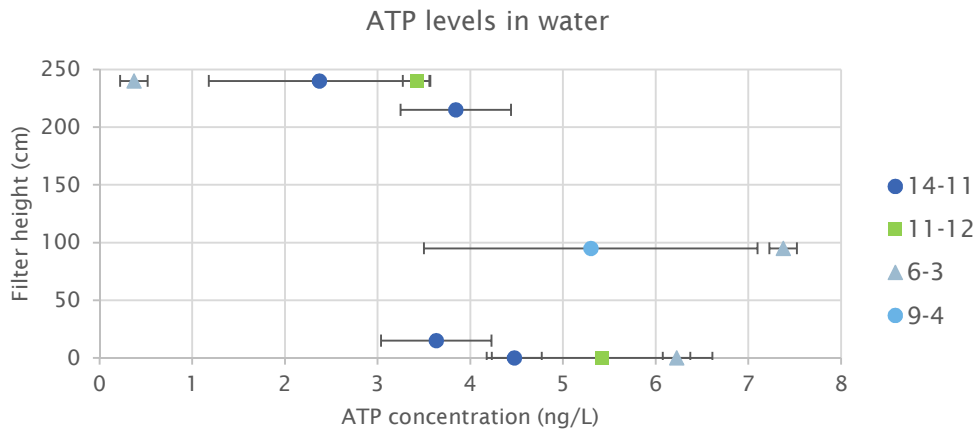


FIGURE 3-1: ATP LEVELS MEASURED IN WATER AT DIFFERENT FILTER HEIGHTS. ERROR BARS CORRESPOND TO SAMPLE STANDARD DEVIATION.

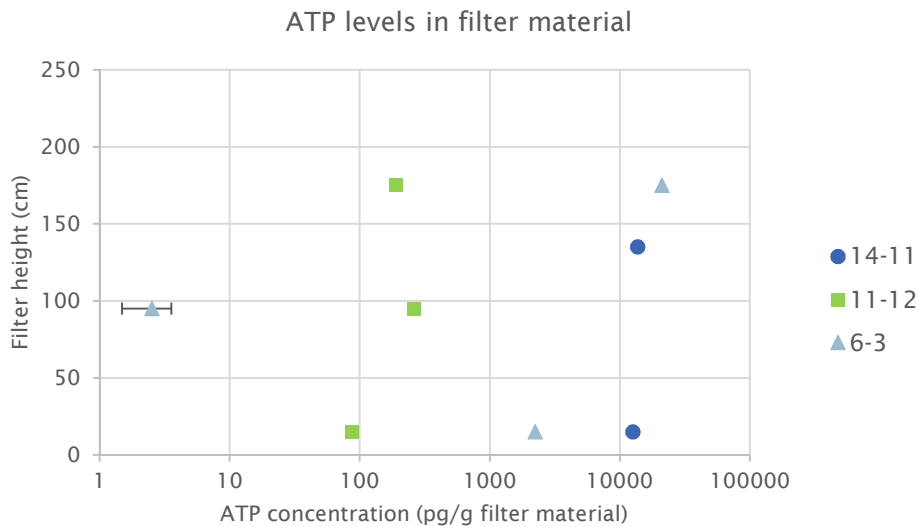


FIGURE 3-2: ATP LEVELS IN FILTER MATERIAL. SAMPLE ERROR VALUES (ERROR BARS) ARE NEGLIGIBLE, EXCEPT FOR THE SAMPLE TAKEN AT 06-03 WITH A VALUE BELOW 10 pg/g FILTER MATERIAL.

It was expected that ATP concentrations would be lower as a result of backwashing the filter. In Figure 3-1 we see that ATP levels range between and 0.4 and 7.4 ng/L, but that samples have considerable measurement uncertainty. Because of this, we are unable to draw conclusions about the spatial distribution of biological material across the filter bed or conclusions about changes of biological activity during the ripening stage of the filter. Figure 3-2 depicts ATP levels found on the filter material, where samples are taken at various heights of the filter. The depicted results indicate a slight decrease in ATP from top to the bottom of the filter bed. Again, caution should be taken to draw conclusions because there is only a limited sample frequency (both in time and in space).

### 3.1.2 DNA analysis of ammonia oxidizing bacteria and archaea by qPCR

To determine the quantity of ammonia oxidizing bacteria (AOB) and archaea (AOA), water and sand samples were taken on four dates: 14 November 2014, 11 December 2014, 6 March 2015, and 9 April 2015. As an example, the results of the sampling campaign on 6 March are presented below (results of the other sampling dates are presented in Appendix II). It has to be noted that the efficiency of the DNA extraction of the anthracite sample was low (one sample < 1 %, another sample an extraction efficiency of 12%), hence hampering the reliability of the calculation of the amount of DNA copies in the original sample (not shown in error bars)..

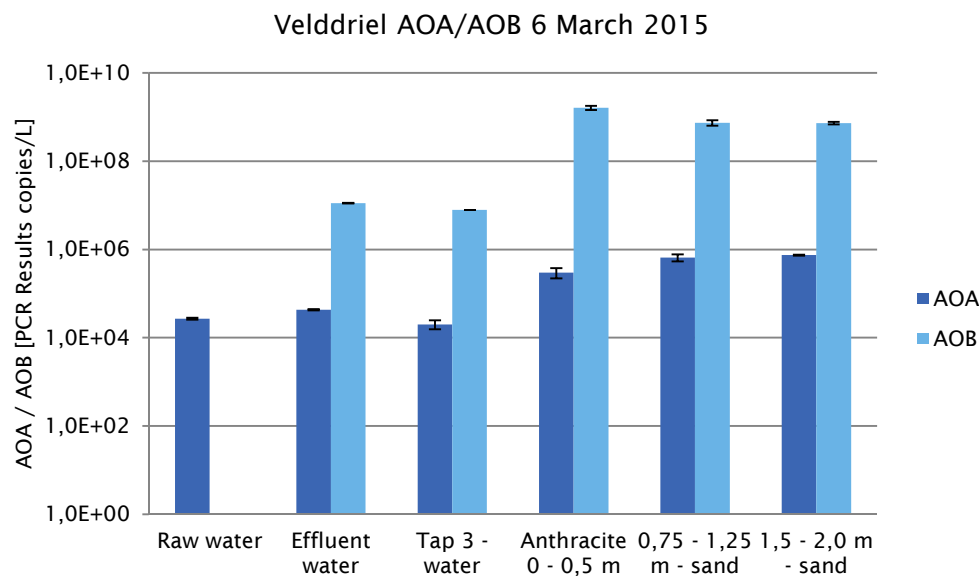


FIGURE 3-3: QUANTITY AMMONIA OXIDIZING ARCHAEA (AOA) AND BACTERIA (AOB) IN WATER AND SAND SAMPLES ON 6 MARCH 2015. NB. RAW WATER SAMPLE WAS NOT ANALYSED FOR AOB.

From Figure 3-3 it seems that the quantity of AOB and AOA in sand samples is in general higher than in water samples. This corresponds to earlier findings of Kramer (2012) who concluded that ATP concentrations were higher and showed less variability in the soil phase compared to the water phase. Note that the amount of copies in the sand layer converted to the amount of copies per unit surface area of the filter material gives an alternative view on the coverage of the filter material surface area by micro-organisms.

The AOA and AOB seems to be evenly distributed over the filter height, while it was expected that most AOB and AOA would be present in the upper layer of the filter (first few centimetres). The even distribution of the experimentally determined values could be explained by the

relatively low running time of the filter (only 3 months). It is possible that the distribution of AOA and AOB will change as a result of filter running time.

In addition, the quantity of AOA seems to be generally lower than the quantity of AOB (approximately a factor  $10^3$  for water samples and a factor  $10^4$  for sand samples).

Although some trends are observed in the results of the AOA and AOB analysis, data obtained in this study is limited to a small amount of samples. More data is required to confirm and generalize the above observations.

## 3.2 Modelled iron, ammonium and manganese removal compared with Velddriel and Holten data

### 3.2.1 Iron and manganese removal: single layer model

Figure 3-4 and Figure 3-5 show simulation results and measurements of the pre-aerated (P.A.) RSF of Velddriel (dual media) and Holten (single medium), respectively. The Holten filter shows a good fit between the model and the measured values of iron(II) and manganese(II) within the filter bed. Note that for the WPB Holten case, filter material has been sampled in order to determine the Freundlich isotherm values (Schoonenberg Kegel, 2015).

The results of WTP Velddriel (Figure 3-4 and Figure 3-5) show that:

- the single layer model fit is poor for the Velddriel filter when the model uses the determined adsorption isotherm values of the middle or lower part of the sand layer for manganese removal. Remarkably, anthracite seems to adsorb manganese(II) quite well, at least considering the filter material is relatively 'fresh' (the filter material had been replaced 3 months before sampling);
- simulations show a delay in iron removal compared to measured values;
- heterogeneous oxidation of iron(II) is amongst others dependent on the adsorbed amount of iron(II) on HFO ( $\text{HFO\_OFe}^+$  and  $\text{HFO\_OHFe}^+$ ), hence starts as soon as these ions get adsorbed (see fig 3-4e). It appears that, as the top layer gets saturated with iron(II) and gets oxidized, the front of adsorbed iron(II) moves deeper into the bed and heterogeneous removal occurs only at the layer beneath the  $\text{Fe(OH)}_3$  oxides. Furthermore, when (iron) heterogeneous removal is taking place, the calculated pH drops considerably but are (yet) not confirmed by measurements since the current measurements of pH do not reach the required accuracy (see fig 3-4c);
- the measured values of iron(II) varies considerably at a height of approximately 2.0 m from the bottom (just below the supernatant layer), while there is some variation of manganese(II) at a filter height of 1.3 m (compare 3-4a and b). This might be attributed to measurement uncertainties due to (a) mixed sampling of the boundary layer between supernatant and (anthracite) filter layer (sample point 5 is located exactly on the boundary of these two layers), or (b) variation in residence times between the instant of sampling and adding acid to stop further oxidation.
- the removal of iron(II) in the supernatant layer looks slightly underestimated by the Velddriel model (fig 3-4a). The lower predicted iron(II) concentrations could be attributed to (a) another residence time distribution than assumed by CSTR modeling or (b) a higher value of the homogeneous oxidation rate constant. Validation with the current data set is limited due to the uncertainty of the height of sampling point (see previous aspect);
- (the modeled) manganese adsorption (fig 3-4f) is pre-dominantly sensitive to the adsorption (isotherm) characteristics, and according to the model equations, also to the heterogeneous manganese oxidation rate constant ( $k_{\text{Mn,het}}$ );

- oxygen decrease is underestimated by the Velddriel model (fig 3-4d). This could be attributed to an underestimated homogenous oxidation (see the measured iron(II) profile), more oxygen consumption by micro-organisms than is assumed (e.g. by nitrification), or a combination of these aspects.

Concluding, a single medium filter model is not the most appropriate solution to simulate dual media filters, because iron but especially manganese sorption characteristics vary along the filter bed height and are related to filter media characteristics (confirmed earlier by e.g. Sharma, Greetham, & Schippers (1999)).

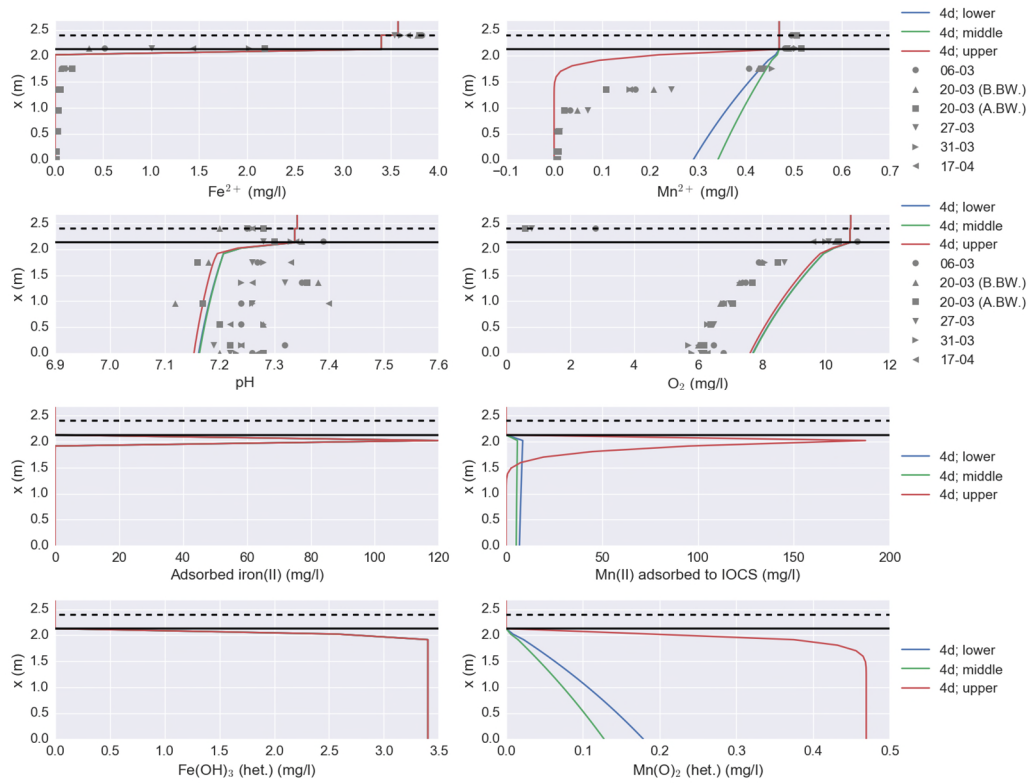


FIGURE 3-4: VELDDRIEL SINGLE LAYER MODEL (DIFFERENT FREUNDLICH PARAMETERS, UPPER LAYER: RED, MIDDLE LAYER: GREEN, LOWER LAYER: BLUE) AND MEASUREMENTS (GREY MARKERS) OVER BED HEIGHT (YAXIS). FIRST 4 ROWS: SIMULATED 4 DAYS OF FILTRATION RUN TIME,

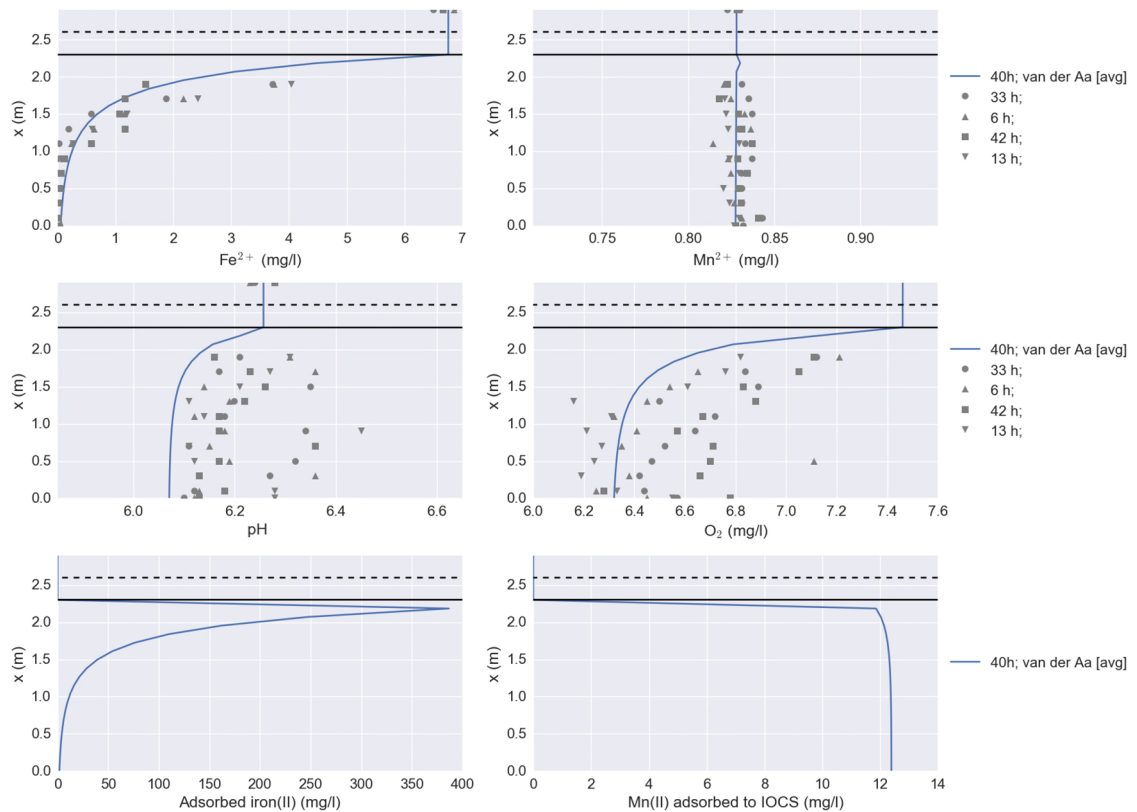


FIGURE 3-5: HOLTEN SINGLE LAYER MODEL (LINES) AND MEASUREMENTS (GREY MARKERS) OF IRON(II) AND MANGANESE (II) CONCENTRATIONS OVER BED HEIGHT (TOP ROW), PH AND OXYGEN (SECOND ROW) AND AMOUNT OF ADSORBED IONS (BOTTOM ROW) SIMULATED AT 40 HOURS AFTER A CLEAN BED START-UP, MAKING USE OF THE NITRIFICATION MODEL WITH AVERAGED VALUES AS ADOPTED FROM VAN DER AA ET AL. (2002).

### 3.2.2 Iron and manganese removal: dual filter media model

Three variations of the dual filter media model have been tested: one with the boundary between anthracite and sand at 0.32 m, another one where the boundary is at 0.43 m and a third with a boundary at 1.0 m. Simulations are executed with a total filter run time of 31 days.

A snapshot of the simulation results with these three different ratios of anthracite versus amount of sand at a filter run period of 2 days are depicted in Figure 3-6, assuming the same heterogeneous manganese oxidation rate ( $k_{Mn,het}=2.4 \cdot 10^{-4} \text{ s}^{-1}$ , see (Davies & Morgan, 1989)) for anthracite and sand (panels a - f) and no heterogeneous oxidation of manganese(II) in the anthracite layer ( $k_{Mn,het,anthr}=0.0 \text{ s}^{-1}$ ) (panels g - i). Figure 3-6, panel d and j show that, counterintuitively, the anthracite layer (iron oxide coated anthracite, IOCA) adsorbs manganese(II) considerably. Note however, that the isotherm adsorption experiments have been carried out with synthetic iron(II) and manganese(II) solutions, but not with a solution where *both* manganese and iron were added. Hence, the model does not incorporate adsorptive competition. Furthermore, notice from panel b that the lower layer seems to adsorb manganese better than the middle layer, but this might be attributed to sample variation in the isotherm adsorption experiments.

When it is assumed that no heterogeneous oxidation of manganese takes place in the anthracite layer, a thick layer of anthracite (e.g. 1.0 m) will have a delaying effect on heterogeneous manganese removal (cf. panel f with panel l of Figure 3-6). Please note furthermore that, due to the low adsorptive capacity of the sand layer for manganese, only heterogeneous oxidation could be responsible for manganese(II) removal.

Especially the slope of the manganese concentration profile in the sand layer region (Figure 3-6, panel b, blue and green line) indicate that,  $k_{het,Mnd}$  for MOCS must be higher than the value reported in literature. Hence, competitive adsorption effects aside, there is an indication that heterogeneous oxidation of manganese(II) in anthracite is weak, but in the sand layer rather strong. A higher rate constant might be attributed to biological activity as suggested by Bruins (2011).

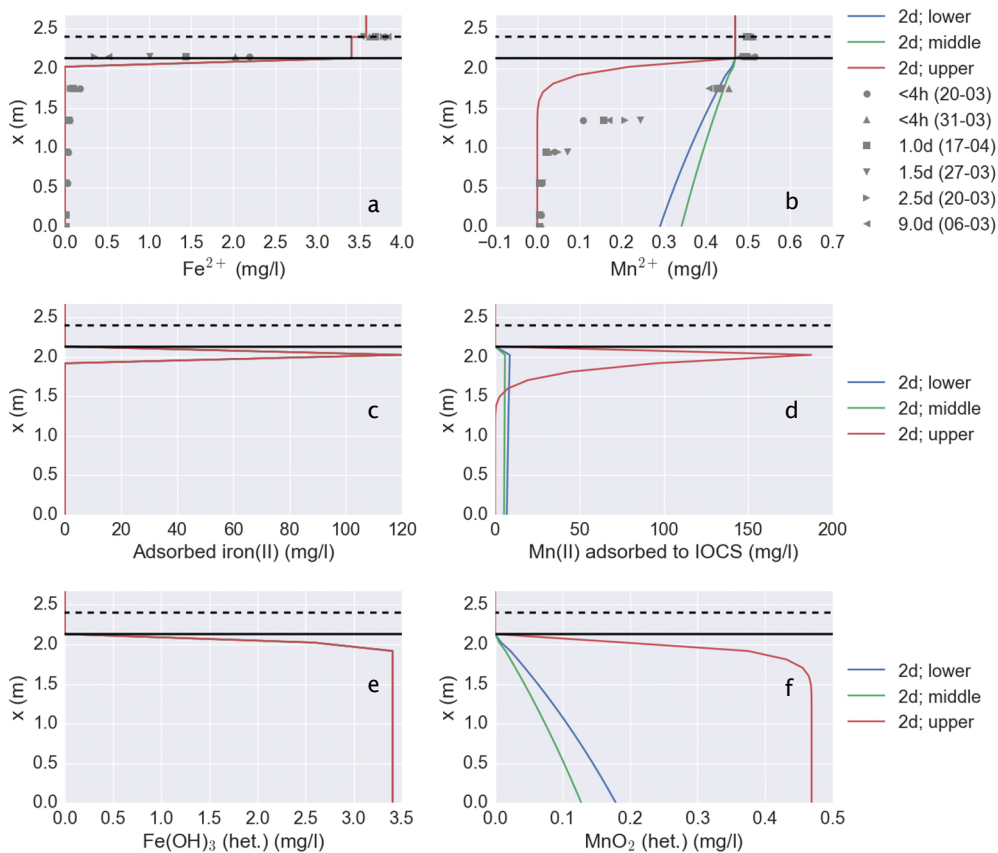
The observation of the influence of  $k_{het,Mnd}$  was an incentive to vary the value of this parameter, results are shown in Figure 3-7. This figure shows that:

- Calibrating  $k_{het,Mnd}$  has a negligible effect on pH and oxygen (panels c-d) and the iron concentration profile (panel a) or the adsorbed amount of iron(II) (panel e) and heterogeneously formed iron oxides (panel g);
- Increasing  $k_{het,Mnd}$  causes a drop in manganese concentration across the bed (panel b), and an increase in the adsorbed amount of manganese (f) and heterogeneously formed amount of manganese oxides (panel h).

From the measured manganese concentration profile and the effects of variation in  $k_{het,Mnd}$  it can be deduced that  $k_{het,Mnd}$  of the anthracite layer is likely to be different (a much lower value) than the value for the sand layer, and that the sand layer has a much higher value ( $k_{Mn,het}=2.0 \cdot 10^{-3} \text{ s}^{-1}$ ) than reported in literature.

The amount of adsorbed iron(II) and manganese(II) and their removal during filter run time, varying the period of the filtration run from 12 hours to 7 days is shown in Figure 3-8. The RSF unit was started in January 2015 and manganese removal was assumed to be at its desired operating value 1 month later. Modeled iron(II) (panel a) shows a sharp decline over a region of a few centimeters throughout the filter run time, whereas the removal of manganese(II) (panel b) occurs more gradually over the filter bed height. Simulation results correspond well for the case that the heterogeneous manganese constant is calibrated:  $k_{Mn,hetero}=2.0 \cdot 10^{-3} \text{ s}^{-1}$  for the MOCS layer and assumed negligible ( $k_{Mn,hetero}=2.4 \cdot 10^{-6} \text{ s}^{-1}$ ) for the anthracite layer, and assuming samples are taken at least one day after backwashing. The simulation show that the start-up of a clean filter bed does not correspond well to the measured samples after backwashing, hence indicating that either backwashing does not remove all adsorbed iron and manganese or adsorption. Notice furthermore that the low value of the manganese heterogeneous oxidation rate constant causes a breakthrough front in the anthracite layer.

In addition, one can see that the sharp (simulated) decline in pH at approximately 1.8 m filter bed height (from the bottom) occurs simultaneously with the removal of iron, corresponding with the release of protons during heterogeneous oxidation. Hence pH seems to be an important indicator of filtration efficiency, but also ammonium may provide additional information about efficiency. pH measurements show large variation among the collected samples, making validation difficult. In addition, there is a mismatch in modeled oxygen decrease which could be attributed to one or more of the following: (i) most importantly, homogeneous oxidation is underestimated, hence pushing the modeled heterogeneous removal front deeper into the filter bed, (ii) oxygen depleted pockets were present in the filter which is not accounted for in the model or (iii) (more) oxygen is consumed by bacteria.



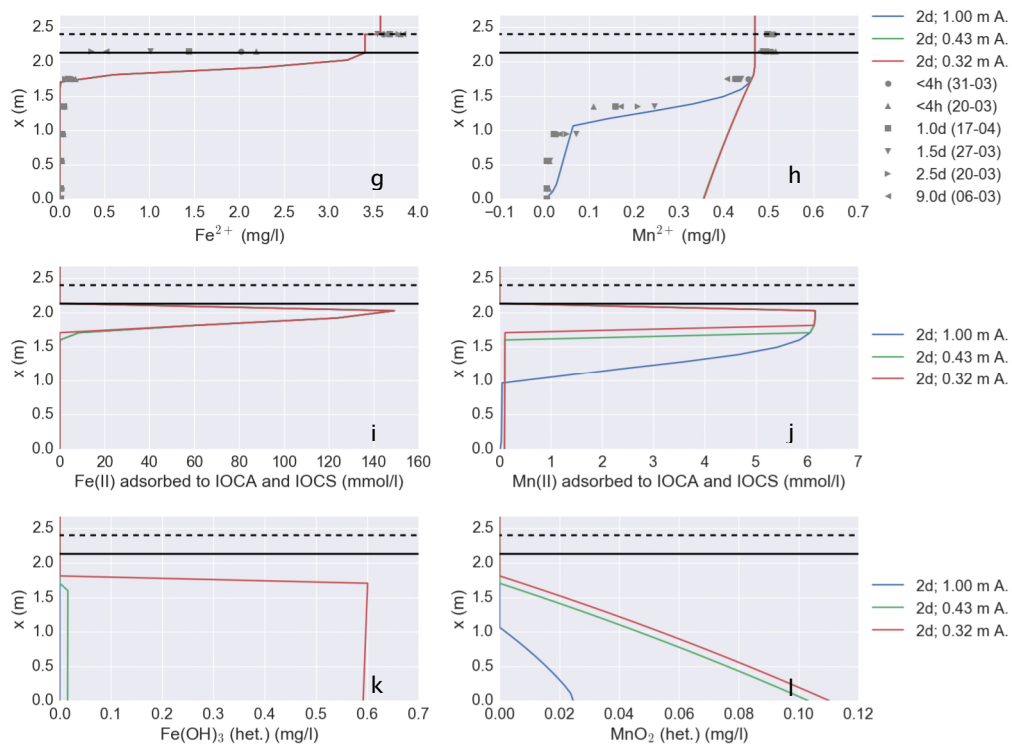


FIGURE 3-6, (A)-(F): SNAPSHOT OF THE RSF MODEL SIMULATION AFTER A FILTER RUN OF 2 DAYS ((A)-(F)) SIMULATED ASSUMING A SINGLE LAYER MODEL (A-F) AND A DUAL LAYER MODEL (G-L) WITH A BOUNDARY

LAYER ([A]NTHRACITE - SAND) AT 0.32 (RED), 0.43 (GREEN) AND 1.0 M (BLUE). MEASUREMENTS ARE DEPICTED WITH GREY MARKERS.

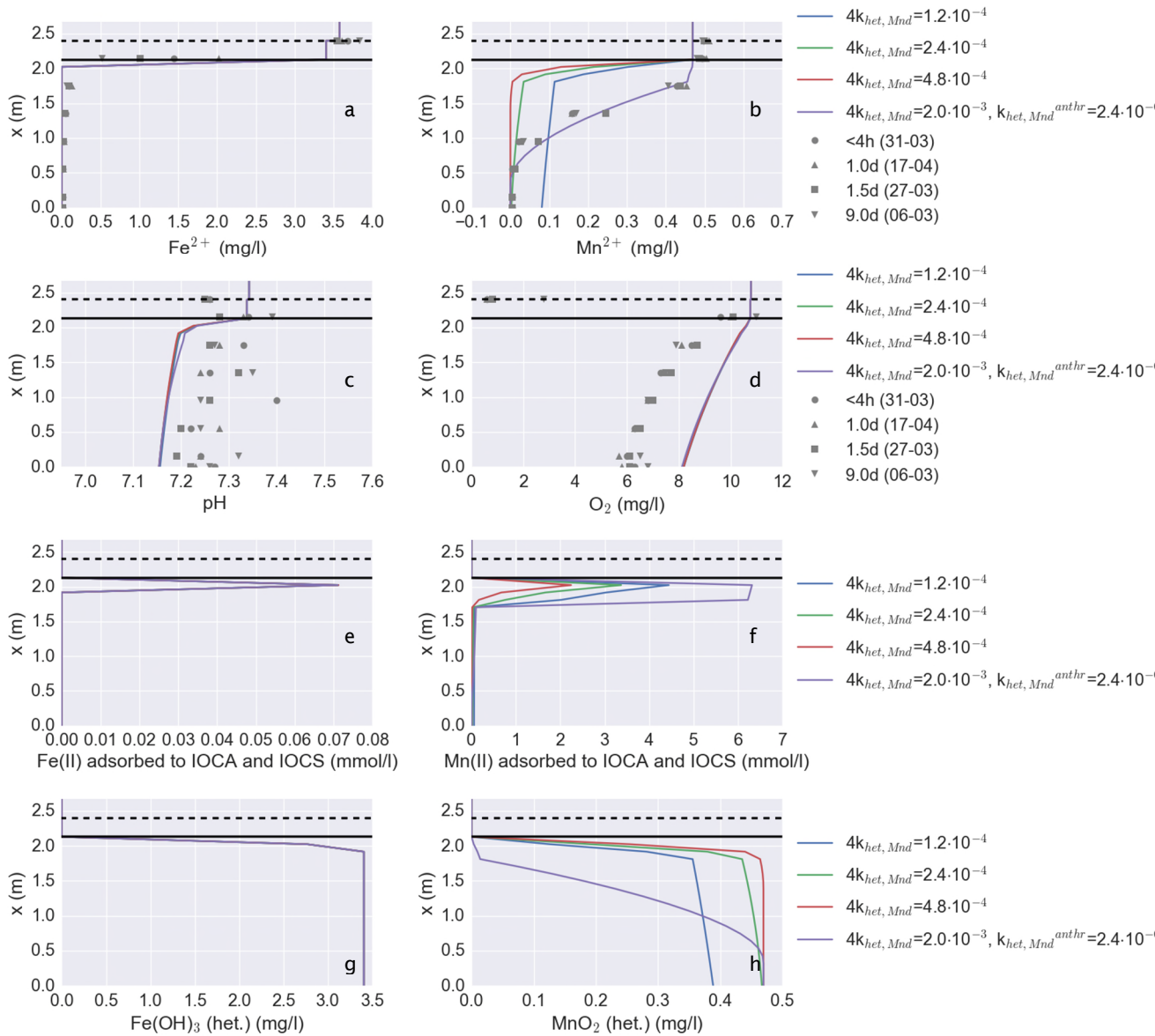


FIGURE 3-7: INFLUENCE OF THE HETEROGENEOUS MANGANESE OXIDATION RATE ON MANGANESE REMOVAL AFTER A SIMULATED RUN TIME OF 4 DAYS, ASSUMING ANTHRACITE- SAND BOUNDARY LAYER AT 32 CM.

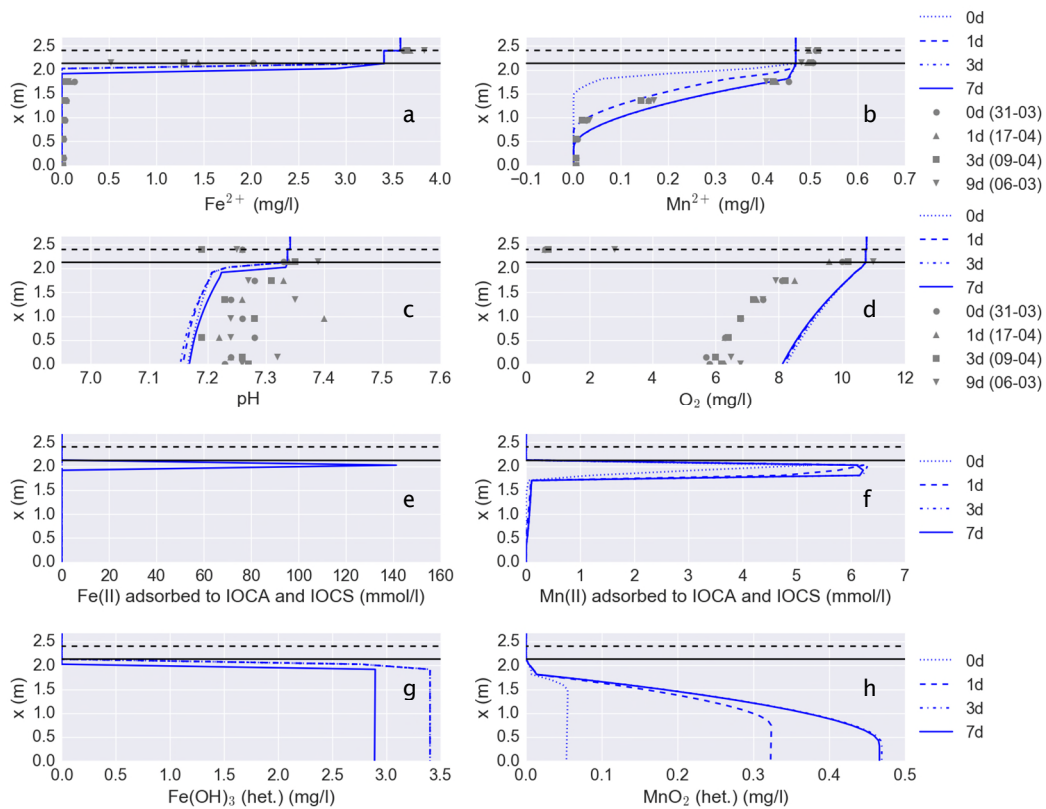


FIGURE 3-8: SIMULATED RSF (BLUE LINES) WITH CALIBRATED  $k_{\text{het},\text{Mnd}}$  (a-h), MEASURED (GREY MARKERS) IRON(II) AND MANGANESE (II) CONCENTRATIONS OVER BED HEIGHT (a,b), PH AND OXYGEN CONCENTRATION (c, d), AMOUNT OF ADSORBED IONS (e, f) AND FORMED OXIDES (g, h) SIMULATED AT DIFFERENT FILTER RUN TIMES IN DAY UNITS (FROM 12H TO 7 DAYS).

### 3.2.3 Iron and manganese removal: influence of filtration velocity and dispersivity coefficient

With model simulations, the filtration velocity and the dispersivity coefficient were varied to study their effect on iron and manganese removal. It is expected that a higher filtration velocity will push the iron and manganese levels deeper into the bed, and will cause a shorter residence time in the filter. A shorter residence time will have a negative impact on homogeneous and heterogeneous removal. Indeed, Figure 3-9 shows exactly what is expected when filtration velocity is increased: less oxidation (well pronounced in the case of manganese heterogeneous oxidation) and therefore a slightly higher pH and oxygen concentration profile (resp. Figure 3-9c and d). Notice furthermore that a higher filtration velocity has an effect on the amount of adsorbed metal ions as well. The effect is most visible with iron(II), where due to the decreased homogeneous oxidation time, more iron(II) is left to adsorb to the filter material. Note that a higher porosity will/ is expected to amount to the same effect as decreasing the filtration flow.

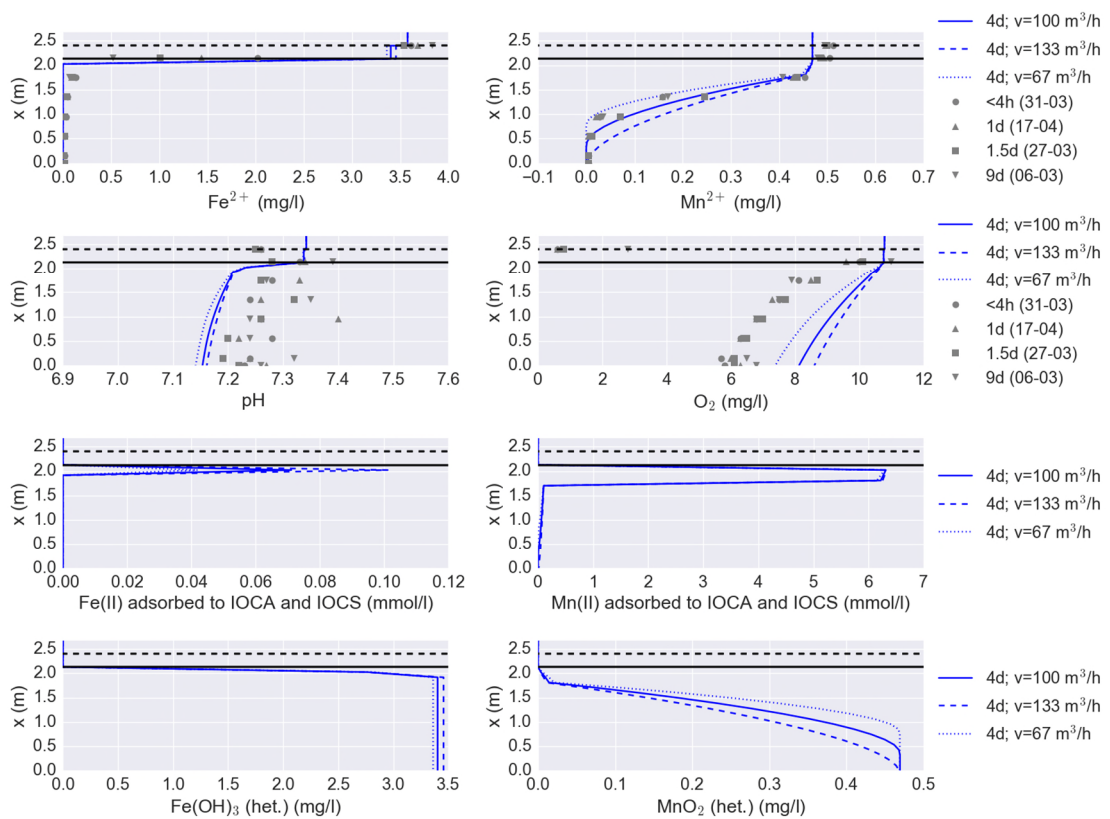


FIGURE 3-9: SIMULATED RESPONSE OVER THE FILTER BED HEIGHT WHEN FILTRATION VELOCITY IS VARIED (SIMULATED FILTRATION TIME: 4 DAYS). FROM UPPER TO LOWER PANELS, 1<sup>ST</sup> ROW: IRON AND MANGANESE CONCENTRATIONS, 2<sup>ND</sup> ROW: PH AND O<sub>2</sub> CONCENTRATION, 3<sup>RD</sup> ROW: AMOUNT OF ADSORBED IRON(II) AND MANGANESE(II) IONS AND 4<sup>TH</sup> ROW: HETEROGENEOUSLY FORMED IRON AND MANGANESE OXIDES.

For the amount of (simulated) dispersivity, the effects on iron and manganese removal are different. Figure 3-10 shows that a higher dispersivity constant causes upward and downward mixing in the filter bed, leading to less adsorption of iron(II) and manganese(II) (e/f) to the filter material and elevated levels of heterogeneous oxidation in the upper anthracite layer. Unless tracer experiments are used to validate dispersion effects, it is generally recommended to keep the dispersion constant at a value smaller than the grid cell size (here < 0.107 m).

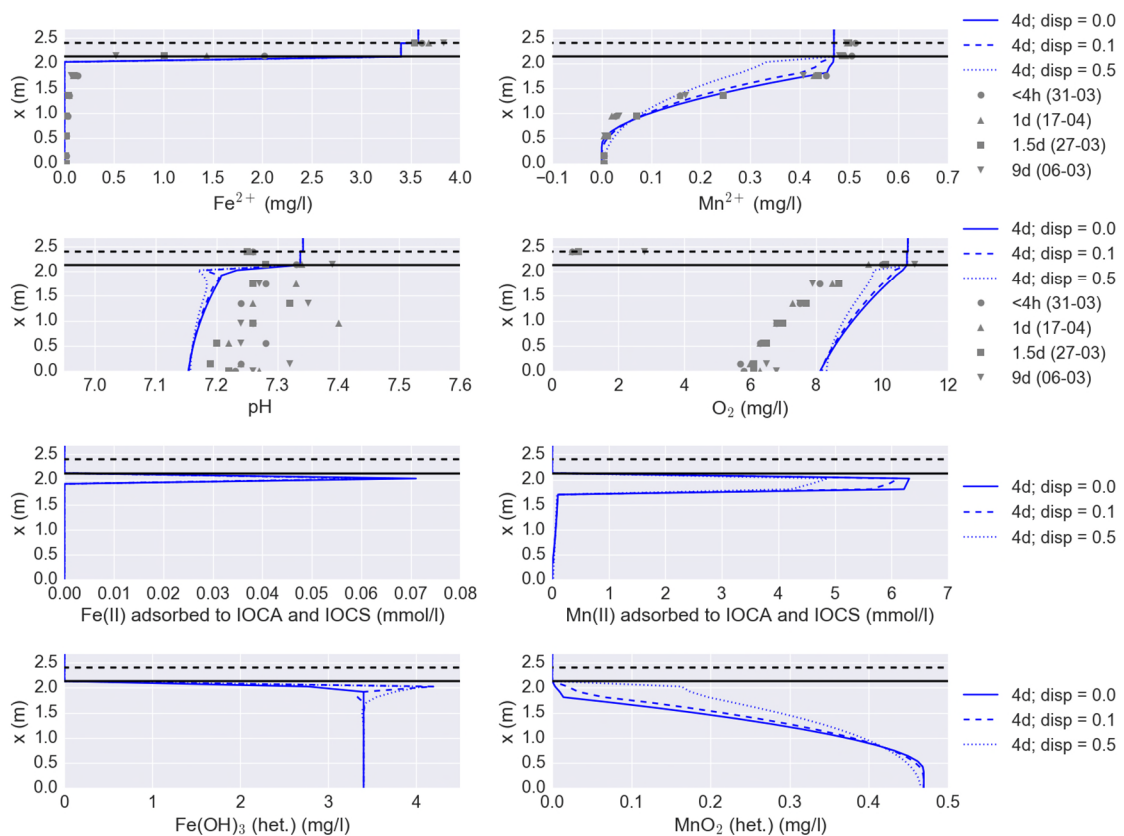


FIGURE 3-10: SIMULATED RESPONSE FOR DIFFERENT VALUES OF THE DISPERSION COEFFICIENT (SIMULATED FILTRATION TIME: 4 DAYS). FROM UPPER TO LOWER PANELS, 1<sup>ST</sup> ROW: IRON AND MANGANESE CONCENTRATIONS, 2<sup>ND</sup> ROW: PH AND O<sub>2</sub> CONCENTRATION, 3<sup>RD</sup> ROW: AMOUNT OF ADSORBED IRON(II) AND MANGANESE(II) IONS AND 4<sup>TH</sup> ROW: HETEROGENEOUSLY FORMED IRON AND MANGANESE OXIDES.

Concluding, the results of the dual media RSF show that there is a need for:

- knowing the sorption characteristics (Freundlich isotherms) for the filter media in a RSF to be able to characterize the effectiveness of iron(II) and manganese(II) removal in the filter bed and determine (calibrate) the heterogeneous manganese oxidation constant;
- alternatively, having enough data (preferably filter bed concentration profiles with registered backwashing times) and a calibration method to fit the model parameters (Freundlich and the (manganese) heterogeneous rate constant) to the measurement data;
- A more detailed (experimental) validation of modelled iron and manganese removal by:
  - having measurements of the sorption characteristics sampled at different heights (at least 2 for each filter medium) during filter run time to gain insight in the relation between filter media variation and influent water quality;
  - (more) accurate measurements of pH at different times during filtration;
  - perform tracer experiments to assess whether there are dispersion effects or whether an ideal plug flow within the filter bed can be assumed;
  - adsorption isotherm experiments with a solution of different ratios of iron and manganese concentrations are to be carried out to determine competitive effects. In addition, kinetic oxidation experiments have to be carried out to validate the heterogeneous removal kinetics.

- the need of measuring redox potential in order to support pH measurements and the amount of oxidation;
- assessing the *modelled* heterogeneous iron and manganese removal with data of a large number of production sites with a balance of filter bed growth, metal ion supply and removal as done in (Beek et al., 2015).

### 3.2.2 Nitrification

30 simulations have been carried out to study the effect of different (nitrification) model parameters on ammonium removal, oxygen consumption and biomass accumulation, see Table 2-5. Rows that are typeset in boldface correspond to

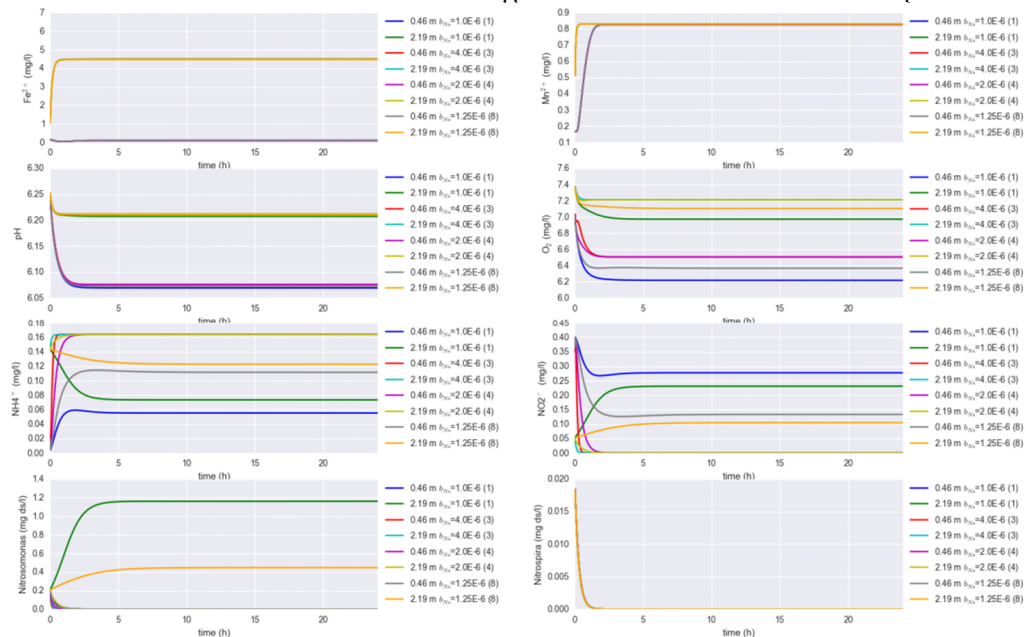


Figure 3-11 to Figure 3-16. Note that we have focused on the removal of ammonium (hence the variation of Nitrosomonas model parameter values), hence we have not studied the effects of Nitrospira model parameters on nitrite removal.

The figures show the following:

- In Figure 3-11 and Figure 3-12, it is shown that with a (most likely) growth rate as reported Table 2-3 (Aa et al., 2002), a lower maintenance rate constant leads to a higher amount of biomass and, consequently a higher consumption and thus more ammonium and oxygen removal. Correspondingly, a higher growth rate constant leads indeed to more biomass, and hence more ammonium removal. Furthermore, notice that with the current parameter value settings, a steady state with respect to the amount of bacteria is reached within 24 hours (Figure 3-11 and bacteria settle in the upper layer of the filter bed. With  $\mu_{\max}^{Nb} = 2.0 \cdot 10^{-5} \text{ s}^{-1}$  and after approximately 6 hours, biomass accumulation apparently reaches a point where ammonium gets depleted in a rate equal to the value of the maintenance rate constant.
- The effect of the maximal growth rate constant of Nitrosomonas  $\mu_{\max}^{Nb}$  (Figure 3-15) seems to be correlated with the Monod constant  $K_S^{Nb}$  (Figure 3-12), although the effect of the growth rate seem to be more pronounced in ammonium levels, nitrite and oxygen consumption.

- The desorption constant  $d_1^{Nb}$  has a large effect on biomass concentration, and hence also on ammonium removal and nitrate conversion. Oxygen consumption is only affected to a small extent (Figure 3-16).

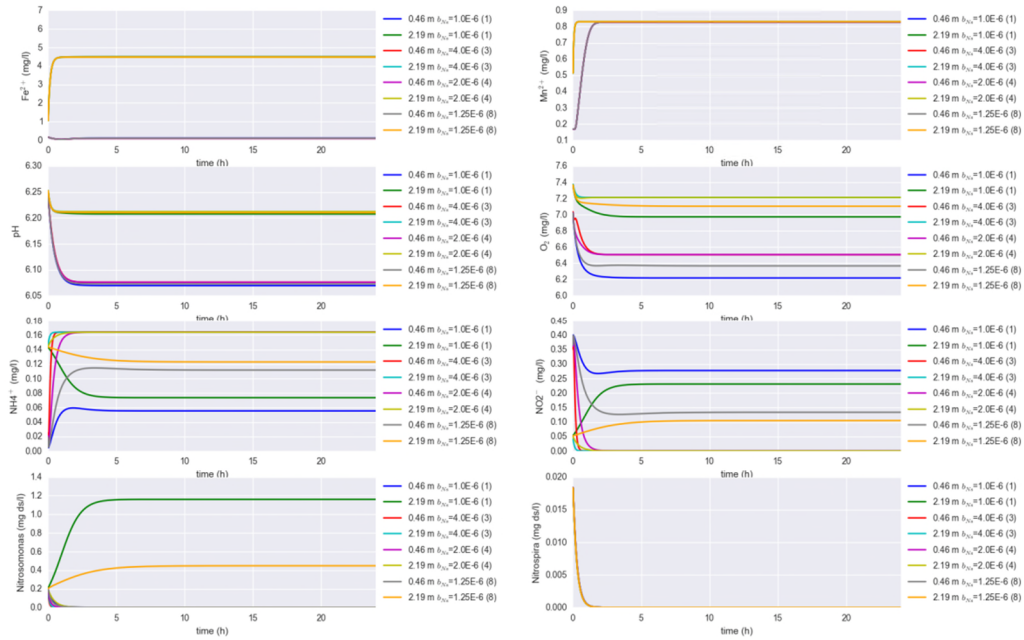


FIGURE 3-11: EFFECT OF THE MAINTENANCE CONSTANT  $B_s$  IN THE GROWTH MODEL OF NITROSOMONAS IN THE FIRST 24H

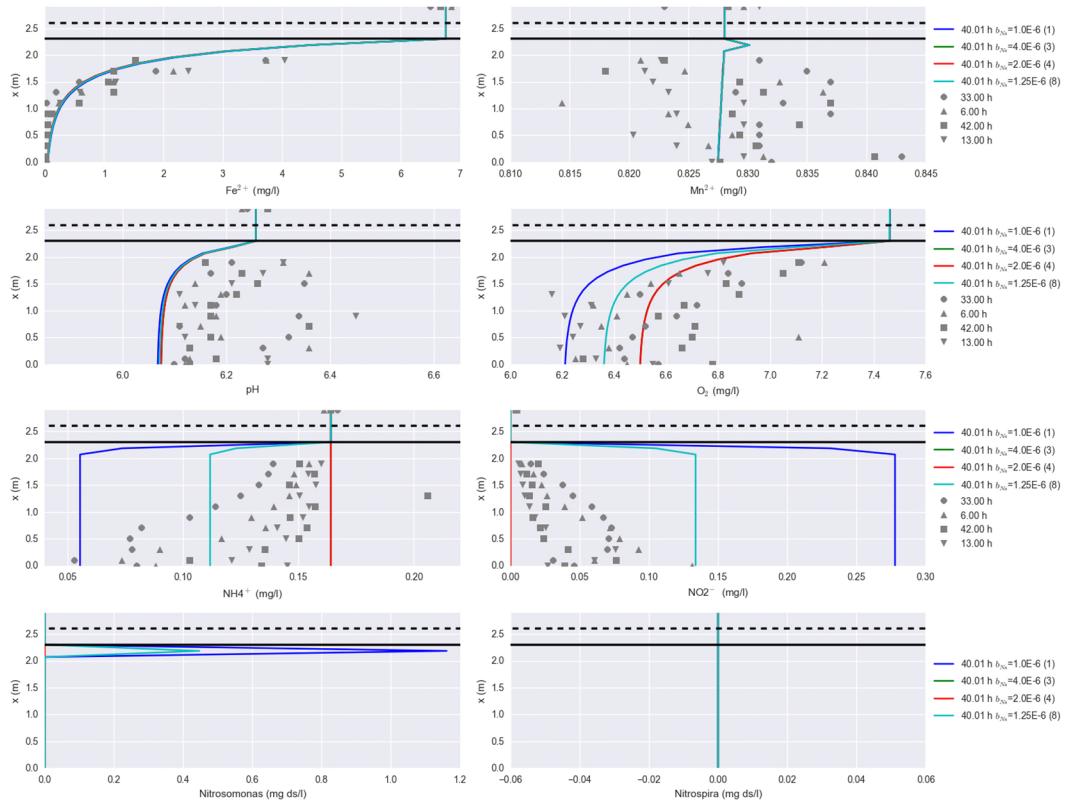


FIGURE 3-12: EFFECT OF THE MAINTENANCE CONSTANT  $b_5$  IN THE GROWTH MODEL OF NITROSOMONAS AT DIFFERENT FILTER BED HEIGHTS

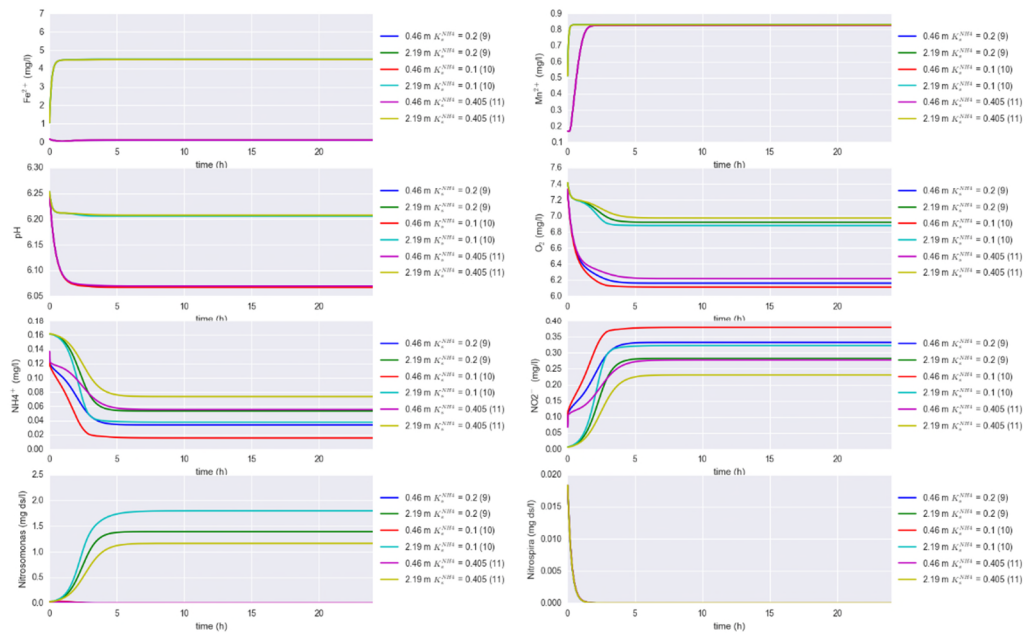


FIGURE 3-13: EFFECT OF THE MONOD CONSTANT ( $K_s$ ) OF THE MICHAELIS-MENTEN CONSUMPTION EQUATION (NITROSOMONAS) IN TIME

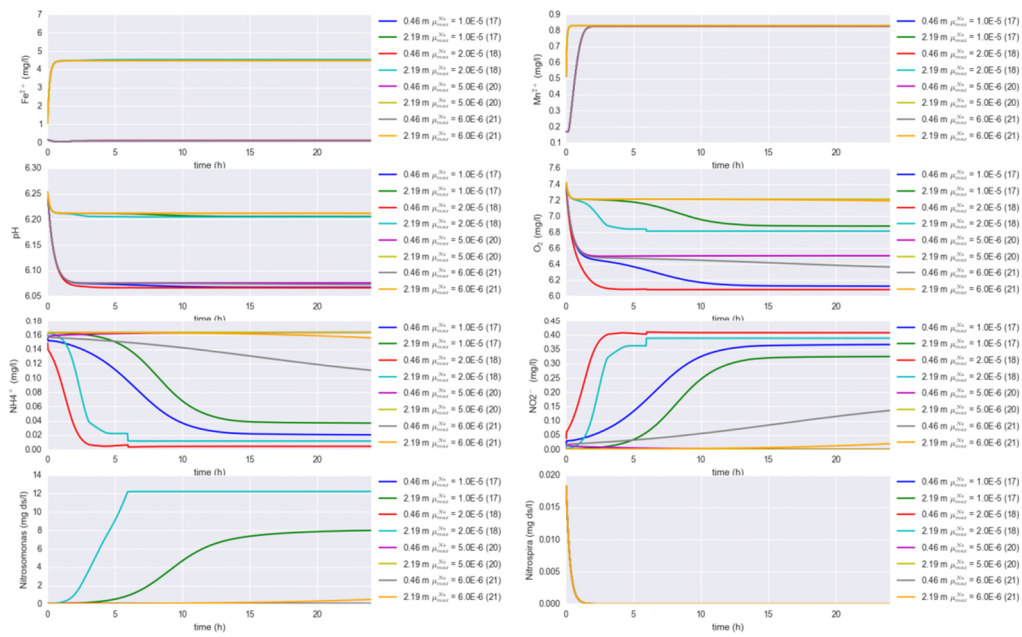


FIGURE 3-14: EFFECT OF THE MAXIMAL GROWTH RATE CONSTANT (NITROSOMONAS) IN TIME

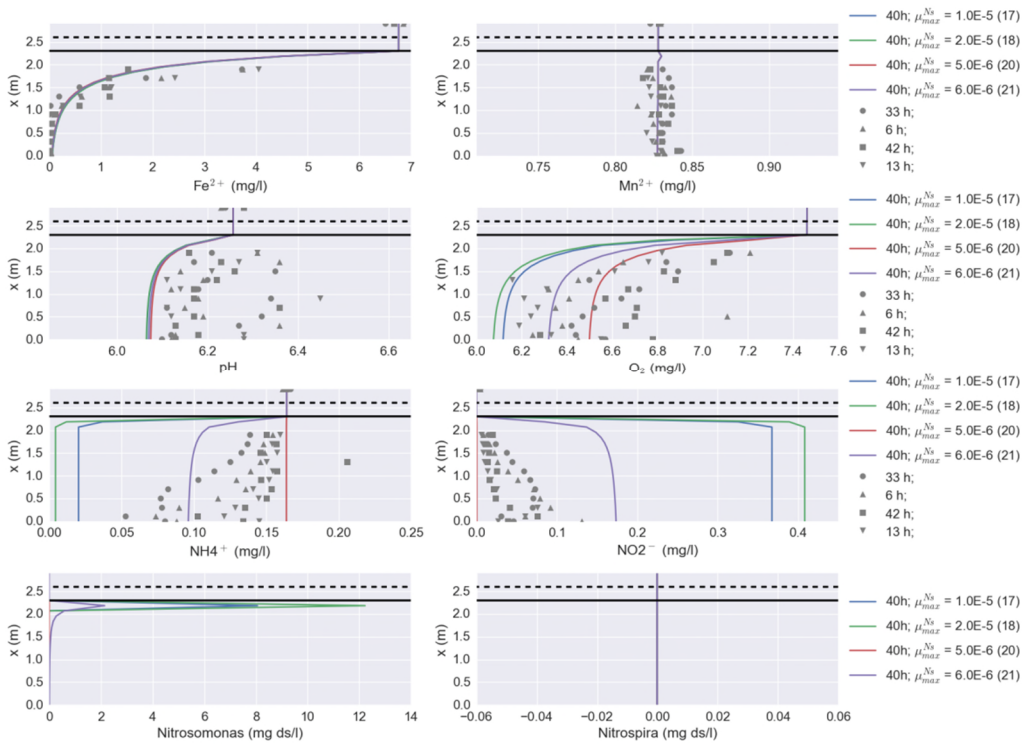


FIGURE 3-15: EFFECT OF THE MAXIMAL GROWTH RATE CONSTANT (NITROSOMONAS) AT DIFFERENT FILTER BED HEIGHTS

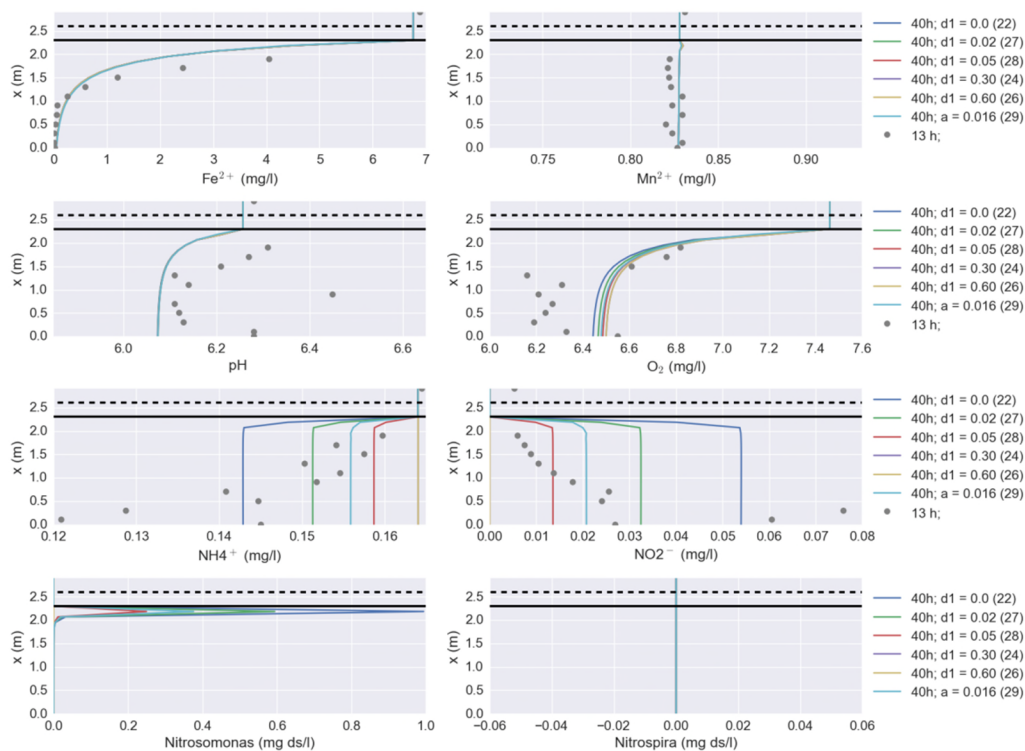


FIGURE 3-16: EFFECT OF DESORPTION CONSTANT ( $d_1$ ) AND DISPERSION ( $a$ ) ON IRON(II) AND MANGANESE(II) REMOVAL (TOP ROW), PH AND OXYGEN (SECOND ROW), AMMONIUM AND NITRITE (THIRD ROW) AND NITROSOMONAS AND NITROSPIRA (FOURTH ROW).

### 3.3 Python-PHREEQC RSF model: preliminary results

The `model.py` file is the result of a first attempt to rewrite the PHREEQC RSF model to the Python framework. The Python-PHREEQC RSF model has been tested for the Holten RSF case, results are shown in Figure 3-17. The figure shows that it is possible to calculate the amount of adsorbed iron(II) and manganese(II), but clearly, the calculated iron(II) and manganese(II) concentration profiles over the bed height are the opposite of what one would expect. Hence, the Python-PHREEQC model needs more work regarding:

- Implementation: (a) numerical dispersion and solving the partial differential equation with an automated cell size calculation (meshing) should preferably be used instead of a fixed cell array and a differencing scheme as implemented here, and (b) it should be checked if PHREEQC consistently reproduces the same values of the differential equations if these are set to zero;
- Computational efficiency: the coupling with PHREEQC takes a lot of computation time (simulating an filtration operational time of 1 hour costed more than 3 hours on a PC, while with the full PHREEQC (transport) model this will take a couple of minutes). The IPHREEQC COM implementation would theoretically speed up<sup>3</sup> the process, but Python – IPHREEQC bindings are still lacking.

<sup>3</sup> The COM module enables calculation in RAM memory, hence avoiding time consuming file input (reading) and output (writing) to ROM (the hard disk).

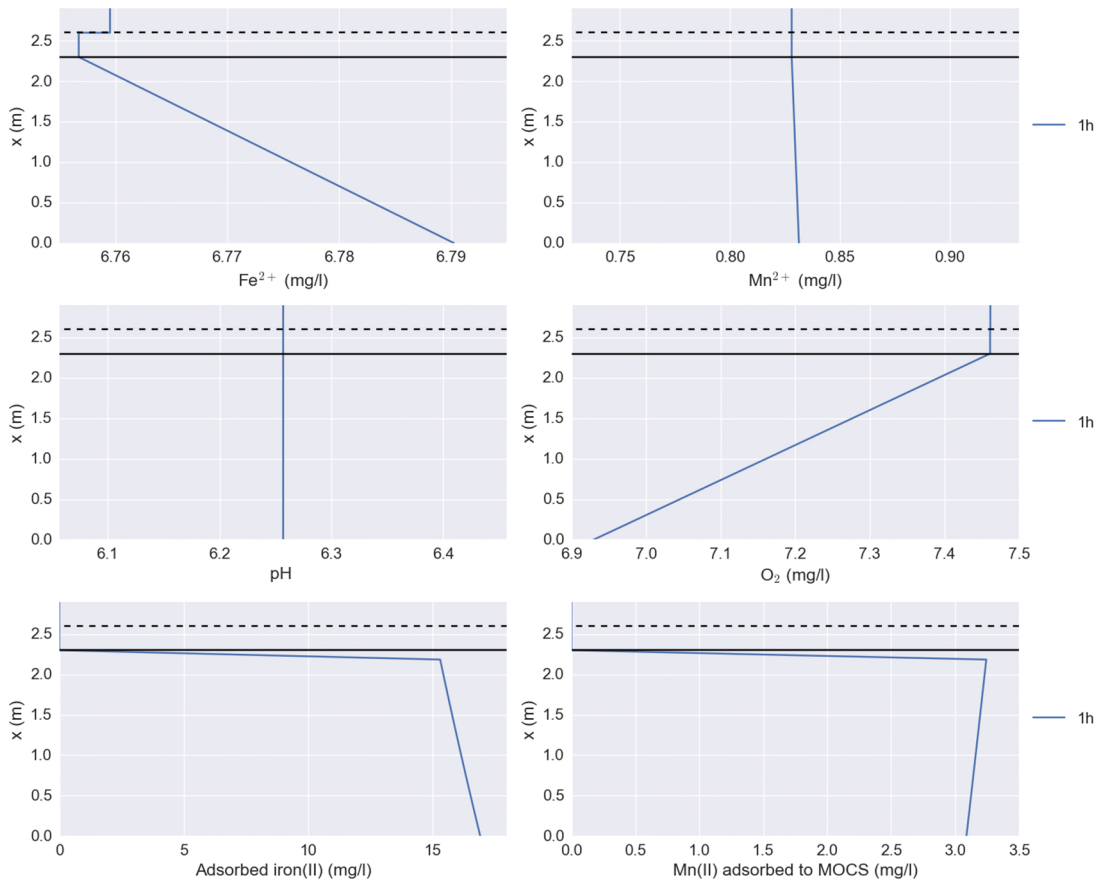


FIGURE 3-17: PRELIMINARY RESULTS FOR IRON AND MANGANESE REMOVAL, USING PHREEQC FOR SPECIATION AND REMOVAL IN THE SUPERNATANT LAYER AND PYTHON FOR REACTIONS AND TRANSPORT IN THE FILTER BED.

## 4 Conclusions and recommendations

### 4.1 Conclusions

A model was developed for iron and manganese removal in a dual media filter which included nitrification. Model simulation results and closer inspection indicate that the model:

- underestimates oxygen decrease in the filter bed. This could be attributed to one or more of the following: (i) oxygen depleted pockets were present in the filter which is not accounted for in the model or (ii) (more) oxygen is consumed by nitrification bacteria;
- the measured ammonium profile is hard to predict with the nitrification model as proposed by Aa et al. (2002);
- is quite sensitive to the duration of filtration run time and the heterogeneous manganese oxidation rate;
- adopts ideal plug flow conditions and filter material grains with the same diameter (i.e. leading to a porosity) and is therefore sensitive to the dispersivity coefficient and the calculated porosity (and hence filtration velocity). Unless tracer experiments are performed that validate dispersion effects, it is recommended to keep the dispersivity coefficient low (typically smaller than the grain diameter (Gitis et al., 2010)) to obtain a close fit.
- fits with measurements when adsorption isotherm parameter values are determined in situ, and when the heterogeneous manganese oxidation in the sand and anthracite layer are calibrated to bed concentration profiles;
- predicts that AOA and AOB will only reside (survive) in the most upper region of the filter bed, consequently leading to ammonium removal in this layer. However, model predictions were not supported by measurements.

Furthermore, it is noted that:

- adsorptive competition between manganese and iron is 'handled' by the procedure to determine adsorption isotherm parameters and subsequently calibrate the heterogeneous constant.
- the effect of backwashing on the microbial population present in the filter bed could not be determined experimentally, but qPCR analysis based on samples collected at one time instant showed that AOA and AOB quantities seemed to be (i) higher in filter media samples compared to water samples, (ii) evenly distributed over the filter and (3) not equal, AOA quantities are much smaller than AOB quantities in the filter. The experimental results indicate that the nitrification model needs to be adjusted to account for a more even distribution of nitrifying bacteria.

### 4.2 Recommendations

The above results can be translated into the following recommendation regarding the improvement of operational efficiency. These are:

**Other process conditions.** Process parameters can be adjusted to improve iron and manganese removal:

- 1) conditioning the aerated water to increase pH (most effective when combining this with measure (2)),
- 2) increasing the residence time in the filter bed by
  - a) increasing the filter bed height or
  - b) lowering the filtration velocity.

Measure (2) may also lead to a lower backwash frequency prolonging the run time of filter material, while measure (1) could lead to more efficient manganese removal.

**Further research.** The current study provided extra insight in the removal mechanisms of iron and manganese in filters and nitrification. A number of aspects still need additional research to assess and confirm the current findings. Therefore, the following recommendations for further research are made:

- Based on the determination of the Freundlich isotherm values of (fresh) filter material, it seems that the adsorptive capacity of iron coated sand substantially exceeds the needed removal capacity of iron and manganese, since iron and manganese removal is complete before the bottom region of the filter bed is reached. However, additional sampling of water and filter material along the filter bed are needed to assess whether this 'redundant' capacity is needed in the long term to prevent early breakthrough of manganese. Redox and more accurate pH measurements would support the contribution due to oxidation. This research will yield valuable information of how the estimation of the expected lifetime of the filter bed can be improved.
- Determine if the adsorption isotherm values of IOCS and IOCA change as a function of operation time. With the sorption characteristics (Freundlich isotherms) for the filter media in a RSF one can characterize the effectiveness of iron(II) and manganese(II) removal in the filter bed and determine (calibrate) the heterogeneous manganese oxidation constant. Alternatively, when having enough measured data (preferably filter bed concentration profiles with registered backwashing times), a calibration method might be able to solve the model parameter estimation problem (i.e. Freundlich and the (manganese) heterogeneous rate constant).
- Adsorption isotherm experiments with a solution of different ratios of iron and manganese concentrations are to be carried out to determine competitive effects. In addition, kinetic oxidation experiments have to be carried out to validate the heterogeneous removal kinetics.
- Tracer experiments with measurements at different depths of the filter bed can be used to determine whether ideal plug flow is a valid assumption for the transport of ions in the filter bed. More attention regarding implementation and computational efficiency should be given to a model framework that is able to describe not only the removal of iron and manganese, but also floc deposit growth, detachment and breakthrough of colloidal particles such that backwashing efficiency and ripening can be related and evaluated to process dynamics (e.g. pressure drop and bed expansion).
- Long term predictions of PHREEQC showed a sawtooth wave pattern in iron, manganese, oxygen, pH and adsorbed ions. More insight is required in PHREEQC to determine what are causing these artefacts in long term predictions of iron/manganese removal, before modeling start-up and backwashing.
- Assess the modelled heterogeneous iron and manganese removal by data of a large number of production sites with a balance of filter bed growth, metal ion supply and removal as done in (Beek et al., 2015), also to further test whether modelling biologically enhanced heterogeneous removal is needed.
- The role of nitrification at start-up and in general was difficult to assess based on the limited data obtained in this study. There is a need to (i) assess AOA and AOB in both

water and filter media samples at three different fixed points in the filter at regular time intervals to enable the exclusion of sample variation and (ii) to differentiate between living and dead cells for both aforementioned aspects to determine which quantity of bacteria are actively involved in the nitrification process.

## 5 Literature

- Aa, L. van der, Kors, L., Wind, A., Hofman, J. A. M. H., & Rietveld, L. (2002). Nitrification in rapid sand filter: phosphate limitation at low temperatures. *Water Science and Technology: Water and Supply*, 2(1), 37–46. Retrieved from <http://ws.iwaponline.com/content/2/1/37>
- Akker, B. Van den, Antoniou, A., Hartog, N., Vries, D., & Hofs, B. (2014). *Iron and manganese removal through subsurface and filtration processes* (No. BTO 2014.047). KWR Watercycle Research Institute: KWR Watercycle Research Institute.
- Beek, C. van, Dusseldorp, J., Joris, K., Huysman, K., Leijssen, H., Schoonenberg-Kegel, F., Vet, W. de, et al. (2015). Contributions of homogeneous, heterogeneous and biological iron (II) oxidation in aeration and rapid sand filtration (RSF) in field sites. *Journal of Water Supply: Research and Technology-Aqua*, jws2015059.
- Bruins, J. (2011). *Improved manganese removal from groundwater*. UNESCO-IHE (PhD proposal).
- Davies, S. H. R., & Morgan, J. J. (1989). Manganese(II) oxidation kinetics on metal oxide surfaces. *Journal of Colloid and Interface Science*, 129(1), 63–77. Retrieved from <http://www.sciencedirect.com/science/article/pii/0021979789904165>
- Gitis, V., Rubinstein, I., Livshits, M., & Ziskind, G. (2010). Deep-bed filtration model with multistage deposition kinetics. *Chemical Engineering Journal*, 163(1), 78–85.
- Jegatheesan, V., & Vigneswaran, S. (2005). Deep bed filtration: mathematical models and observations. *Critical reviews in environmental science and technology*, 35(6), 515–569.
- Kramer, F. (2012). *Removal of Organic Micro Pollutants in Batch Experiments Mimicking Riverbank Filtration*. TU Delft, Delft University of Technology.
- Magic-Knezev, & Kooij, D. van der. (2004). Optimisation and significance of ATP analysis for measuring active biomass in granular activated carbon filters used in water treatment. *Water Research*, 38, 3971–3979.
- Maroudas, A., & Eisenklam, P. (1965). Clarification of suspensions: a study of particle deposition in granular media: Part I—Some observations on particle deposition. *Chemical Engineering Science*, 20(10), 867–873. Retrieved from <http://www.sciencedirect.com/science/article/pii/0009250965800835>

- Rietveld, L. C., Helm, A. van der, Schagen, K. van, Aa, R. van der, & Dijk, H. van. (2008). Integrated simulation of drinking water treatment. *Journal of Water Supply: Research and Technology - AQUA*, 57(3), 133–141. doi:10.2166/aqua.2008.098
- Schoonenberg-Kegel, F. (2013). *Optimization of the iron removal in rapid sand filters. Increase of the heterogenic iron removal by the reduction of the supernatant level.*
- Sharma, S., Greetham, M., & Schippers, J. (1999). Adsorption of iron (II) onto filter media. *Aqua*, 48, 84–91.
- Teunissen, K. (2007). *Iron removal at groundwater pumping station Harderbroek.* Delft University of Technology.
- Vries, D., & Akker, B. v.d. (2013a). *Iron removal, water and sand in water treatment. Sensitivity analysis and a case study of heterogeneous iron removal at WTP Holten* (No. BTO 2013.207(s)). KWR Watercycle Research Institute.
- Vries, D., & Akker, B. van den. (2013b). *Iron removal in rapid sand filtration: modelling results. Sensitivity analysis and a case study of heterogeneous iron removal at WTP Holten.* (No. BTO 2013.207(s)). KWR Watercycle Research Institute.
- Vries, D., Bertelkamp, C., Akker, B. v. d., & Hofs, B. (2016). *Iron and manganese removal: recent advances in modelling treatment efficiency by rapid sand filtration* (No. BTO 2016.015). KWR Watercycle Research Institute.
- Willemse, R. J. N., & Dijk, J. C. van. (1994). Modelling of the degradation of AOC in biological active filters (Modellering van het AOC-afbraakproces in biologisch actieve filters). *H2O*, H2O (Vol. 27, pp. 34–40). KNW.

# Attachment I PHREEQC code blocks

## Dual media filtration and nitrification

For the dual filter media model, Hfo\_anthr\_w is introduced as a surface species representing the anthracite layer, i.e. the upper layer of the filter bed (Figure I-1). IOCS (iron coated sand) is still represented by HFO\_wOH (hydrous ferric oxides) and is defined to reside in the lower region of the filter bed (Figure I-2).

### Dual media filtration model, PHREEQC code

```

SURFACE_MASTER_SPECIES
  Hfo_s  Hfo_sOH
  Hfo_w  Hfo_wOH
  Hfo_anthr_w  Hfo_anthr_w

SURFACE_SPECIES
  Hfo_anthr_w = Hfo_anthr_w
  log_k  0.0

  Hfo_anthr_w + .540Fd+2 = Hfo_anthr_wFd+2
  -no_check
  -mole_balance Hfo_anthr_wFd+2
  # Measured at KWR:
  log_k -2.7652 # upper, pH 7.35, 1/n = 0.540

  Hfo_anthr_w + .814Mnd+2 = Hfo_anthr_wMnd+2
  -no_check
  -mole_balance Hfo_anthr_wMnd+2
  # Measured at KWR:
  log_k -2.689 # upper, pH 7.35, 1/n = 0.814

  Hfo_wOH + .225Fd+2 = Hfo_wOHFd+2
  -no_check
  -mole_balance Hfo_wOHFd+2
  # Measured at KWR
  log_k -4.8335 # middle, pH 7.35, 1/n = 0.225

  Hfo_wOH + .369Mnd+2 = Hfo_wOHMnd+2
  -no_check
  -mole_balance Hfo_wOHMnd+2
  # Measured at KWR
  log_k -3.622 # middle, pH 7.35, 1/n = 0.369

```

FIGURE I-1: PHREEQC CODE BLOCK FOR INITIALIZING TWO FILTER MEDIA PHASES (BEFORE THE DEFINITION OF THE KINETICS AND SOLUTION BLOCK)

```
SURFACE 1-4 # upper layer region: SBL (0.0m) to 0.43 m
        equil solution 21
        Hfo_anthr_w Ferrihydrite eq 1 5.33e4
        -no_edl

SURFACE 5-20 # lower (IOCS) layer region
        equil solution 21
        Hfo_w Ferrihydrite eq 1 5.33e4
        -no_edl

TRANSPORT
        -cells                20
        -lengths              0.1065
        ...

END
```

FIGURE I-2: PHREEQC CODE BLOCK (AFTER THE KINETICS BLOCK), SPECIFYING THE REGIONS AND FILTER MEDIA PHASES OF THE TWO FILTER LAYERS AT WPB VELDDRIEL

### Nitrification

Figure I- shows the code excerpt for initializing the kinetic reactions of Nitrospira and Nitrosomonas. Species and reactions are defined in the PHREEQC database file.

```
EQUILIBRIUM_PHASES 1-20
Ferrihydrite 0 25000
Nitrosomonas 0 .02 # 1 'mole' = 1 g/m^3
Nitrospira 0 .02 # 1 'mole' = 1 g/m^3

SOLUTION 21
units mmol/L
temp 10
<...>

KINETICS 1-20
Nitroso_growth
  -formula NitroSomonas 1000 # 1 # elevated from 1 to
    1000 to speed up the process
  -parms 2.0E-7 0.6E-5 0.405 0.05
  -step_divide 1e-3

Nitroso_removal
  -formula NamH4 -1 O2 -1.5 NniO2 1 H2O 1 H 2
  -parms 0.12 0.6E-5 0.405 0.05
  -step_divide 1e-3

Nitro_growth
  -formula NitroSpira 1000 # 1 # elevated here (see earlier remark)
  -parms 1.0E-6 3E-6 0.0 0.05
  -step_divide 1e-3

Nitro_removal
  -formula NniO2 -1 O2 -0.5 NO3 1
  -parms 0.05 3e-6 0.05
  -step_divide 1e-3
```

FIGURE I-3: PHREEQC CODE TO INITIATE PARAMETER VALUES FOR NITRIFICATION.

Part of transport model in Python, linked to PHREEQC for speciation

```
### Under construction: Holten pre-aeration filters as test case

from subprocess import call
from matplotlib import mlab
import numpy as np
from scipy.optimize import brentq # root finding module
import matplotlib.pyplot as plt

def constructPhreeqC(pH, O2, Fd, Mnd, alk, pe, Fehom=0, Mnhom=0,
Feads=0, Mnads=0, Fehet=0, Mnhet=0):

    template = open('template_HVF_bk.phrq', 'r')

    dFd = -Fehom - Feads

    dMnd = -Mnhom - Mnads

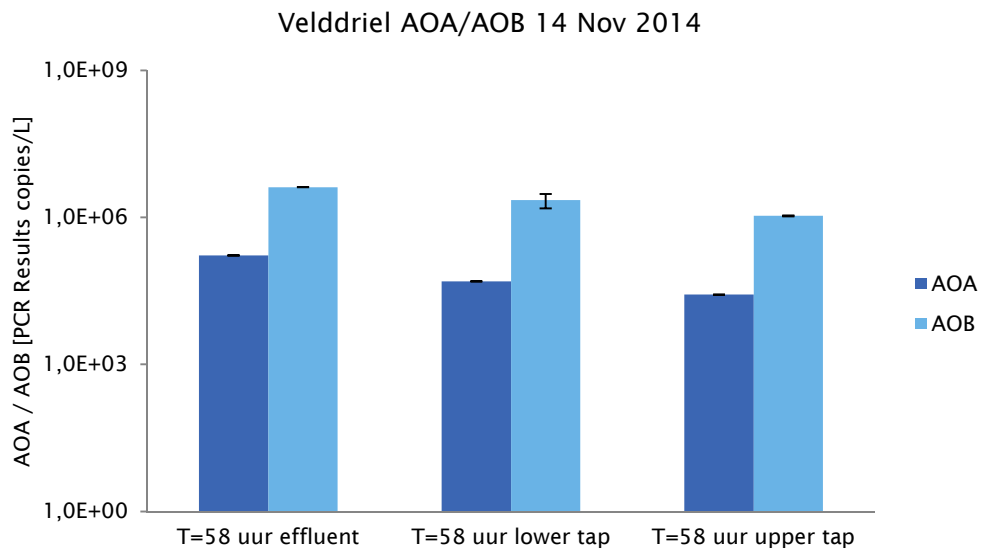
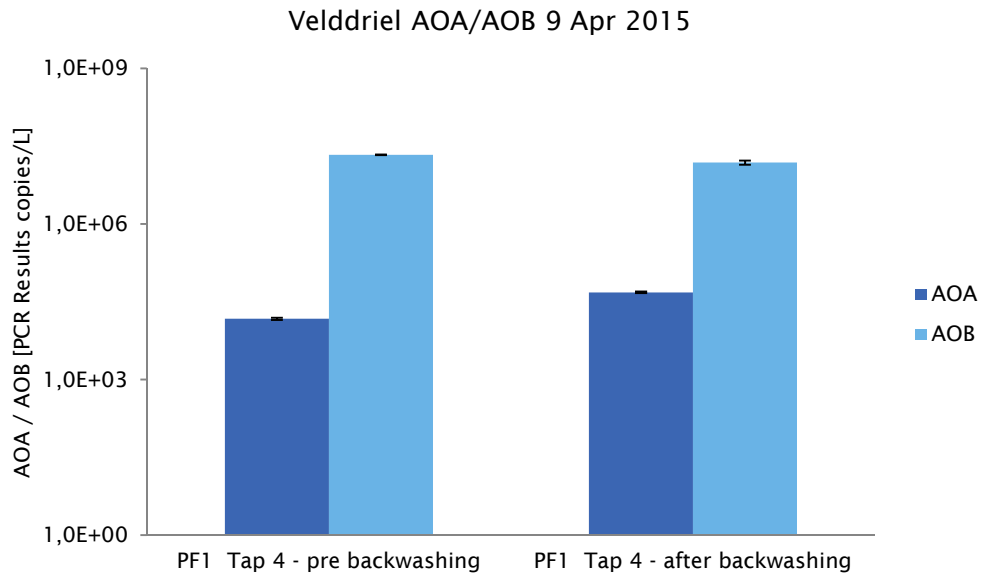
    dO2 = -.25*(Fehom+Fehet) - .5*(Mnhom+Mnhet)

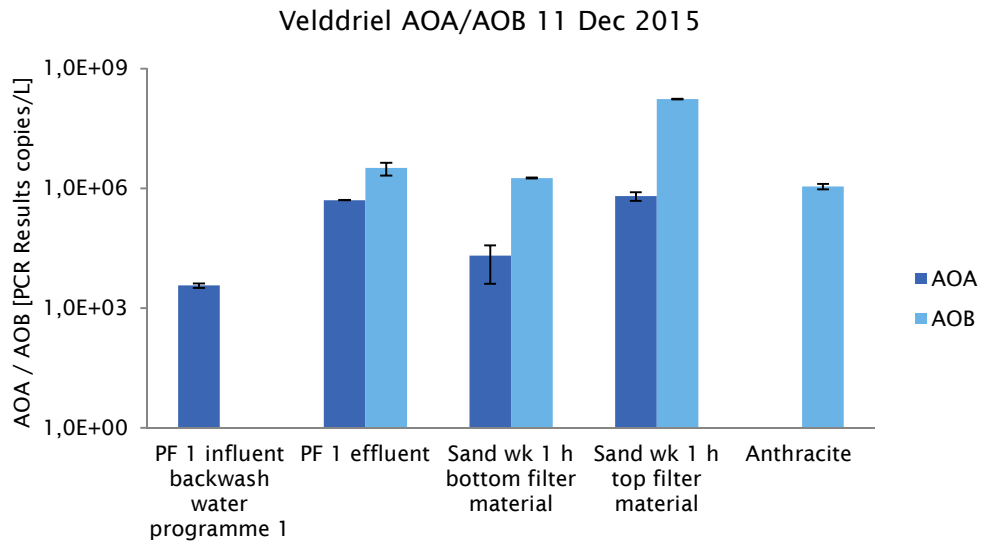
    dH = 2.0*(Fehom+Mnhom+Mnhet) + Feads + Fehet
```

FIGURE I-5-3: PART OF TRANSPORT MODEL IMPLEMENTED IN PYTHON.

# Attachment II Additional figures

## AOA and AOB analysis





# Attachment III Additional figures evolution of iron and manganese removal

## Velddriel, single medium filter model

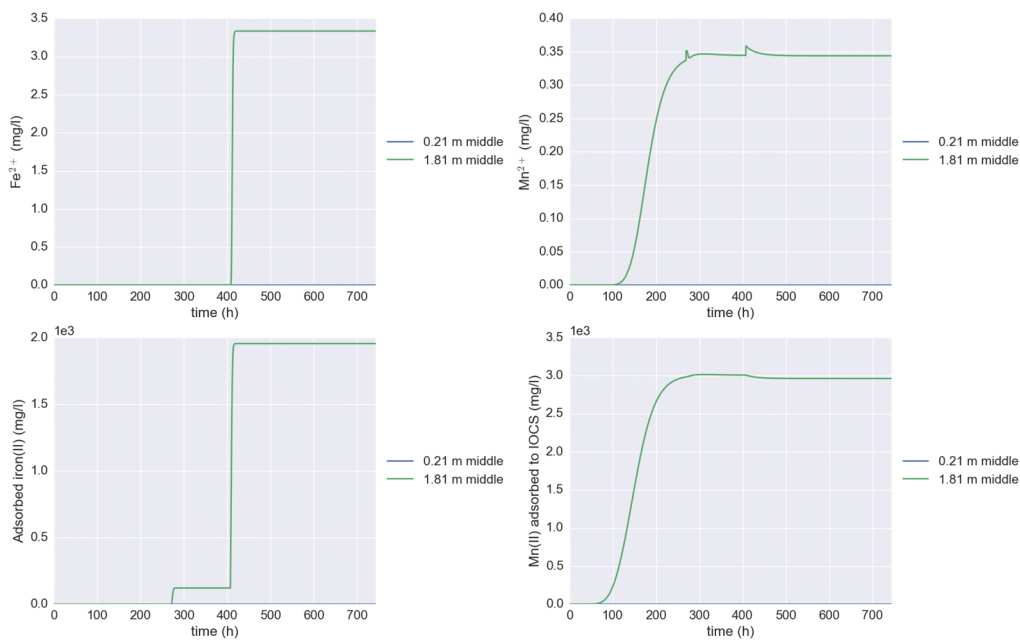


FIGURE ATTACHMENT III-1 : SIMULATED BREAKTHROUGH OF IRON AND MANGANESE AT 0.21 M TO 1.81 M (HEIGHT MEASURED FROM THE BOTTOM).

**Velddriël, double media filter model**

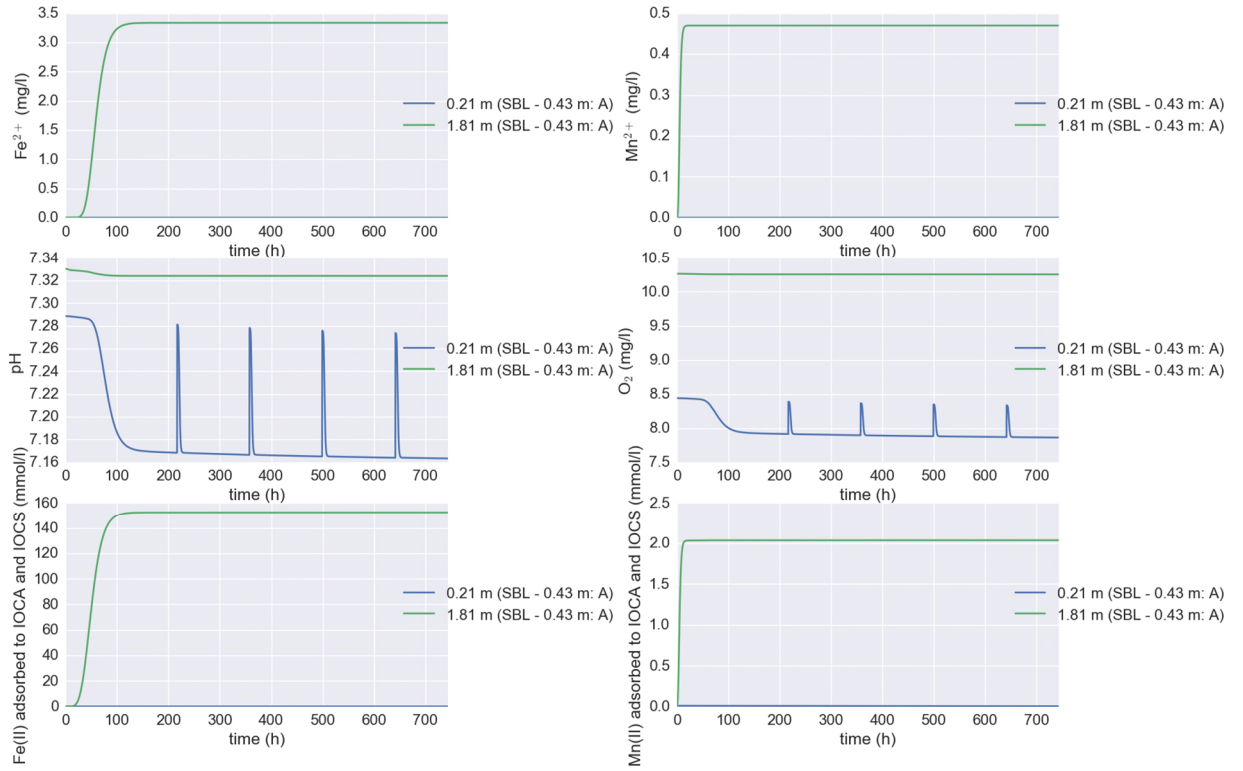


FIGURE ATTACHMENT III-2: SIMULATED BREAKTHROUGH FOR DUAL MEDIA FILTER MODEL OF IRON AND MANGANESE AT 0.21 M TO 1.81 M (HEIGHT MEASURED FROM THE BOTTOM) WHEN THE BOUNDARY BETWEEN ANTHRACITE AND SAND IS 0.43 m.

Holten, dynamic evolution of filtration

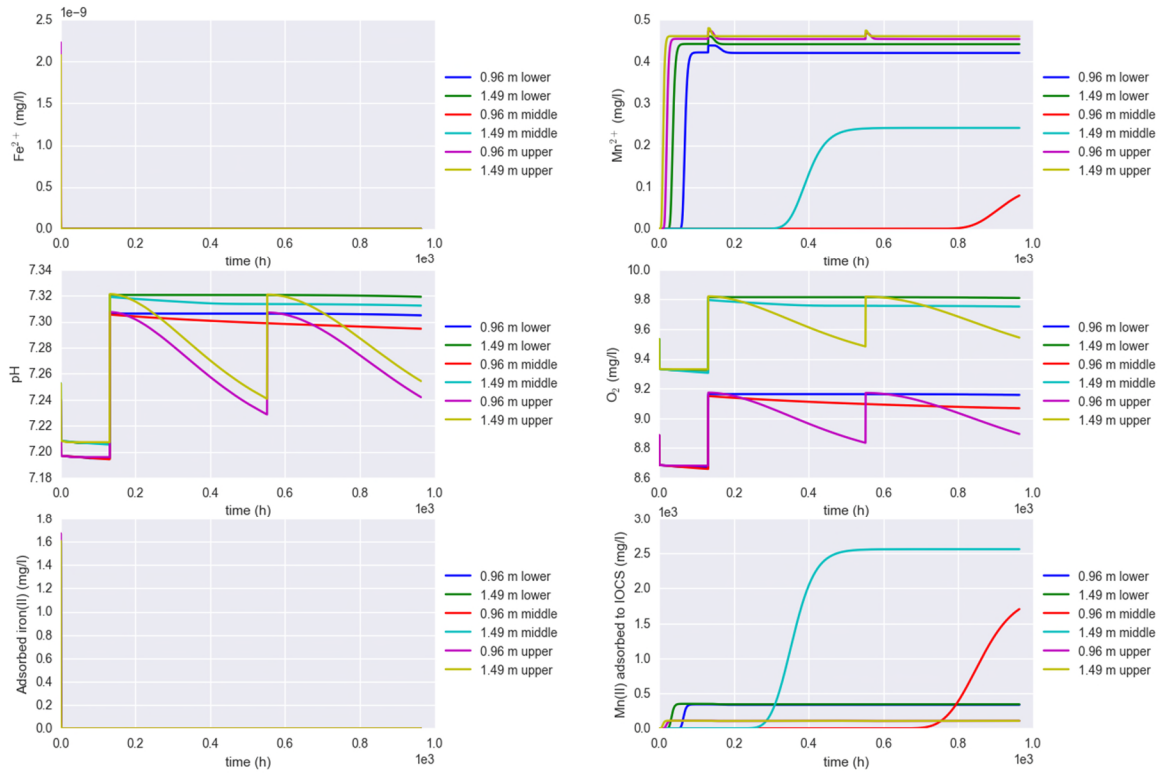


FIGURE ATTACHMENT III-5-4: MODEL RESULTS AT EQUILIBRIUM WITH ADSORPTION ISOTHERM VALUES (LOWER, MIDDLE AND TOP LAYER) AT DIFFERENT FILTER BED DEPTHS (0.96 AND 1.49 m).